MSc Environomical Pathways for Sustainable Energy Systems - SELECT

MSc Thesis

Simulation and Optimization of a Solar Driven Air Conditioning System for Indian Cities

Author:

Dev Sharma

Supervisors:

Principal supervisor: Dr. Elisabet Mas de les Valls, UPC Barcelona

Partner co-supervisor: Dr. James Spelling, KTH Stockholm

Industrial supervisor: Dr. Sanjay Vijayaraghavan, SIEMENS, Bangalore

July, 2012

Acknowledgement

The research for this thesis was conducted at SIEMENS Corporate Research Center, India during an Internship from February 2013 to June 2013. This project was a brainchild of Dr. Sanjay Vijayaraghavan. His persistent dedication towards this project, in spite of innumerable challenges could not be thanked in words. I take this opportunity to thank him for his constant guidance during the project as a supervisor.

I would also like to thank Dr. James Spelling for his constant supervision and support with whatever issues I had with TRNSYS software. James is the only person I know who possesses such knowledge of the software TRNSYS. Hence without a doubt, I can credit him for solving all my doubts about the software.

Dr. Elisabest Valls, my UPC supervisor has also been an integral part of this process. Thank you. This study would not have been possible without each of my three supervisors, but they are not the only people I would like to thank. I would like to thank my family for forever being by my side, even during the worst of times. I would also like to thank my colleagues at SIEMENS (especially Dr. Ramsatish) for their friendly advices during the project.

This thesis is a part of SELECT erasmus mundus master's course in sustainable energy, through which I haven't just gained knowledge in the field of sustainable energy systems but have had the pleasure of spending two years with some of the best people from all over the world. Thank you guys for making this masters a pleasurable experience.

Executive Summary

Conventional air-conditioners need high grade energy i.e. electricity, which in India, is primarily produced from fossil fuels. In spite of several emission restraints exercised by many countries under Kyoto protocol, energy consumption and pollution levels are higher than ever. Therefore, an assessment from the ecological point of view needs to be implemented as the greenhouse gases effect remains a threat to the environment. India is a booming economy with not enough installed power to supply the growing demand. This shortage of electricity results in frequent power cuts, even in the metropolitan cities. In summers, the cooling load of buildings increases due to high ambient temperature. It is during the same time that available solar is at its peak. These are some of the motivations behind usage of solar energy for air conditioning of buildings. Solar cooling technology provides an important contribution to both economical and ecological energy supply.

The aim of this study was to simulate and optimize a solar based absorption system for Indian conditions. Four cities were selected such that they have different incident solar radiation and climatic region. Since Meteonorm data files are not available for all locations, the availability of city's data file was also considered during selection. Meteonorm files are used to simulate the ambient conditions for a location in TRNSYS simulations. Energistic SunTrac27 was selected as the solar collector for this study based on efficiency comparisons.

Standard configuration for the building and comfort conditions was setup based on ASHRAE standards. The cooling loads were estimated with the standard configuration for selected cities. The parametric analysis was conducted to study the impact each of infiltration, ventilation, comfort conditions, heat gains, and other simulation conditions on the cooling load. It was observed that the months which have highest ambient temperature for the selected cities also happen to be the ones with the highest cooling loads. This was because even if solar radiation was not the only parameter affecting the cooling load, it was certainly the only variable for an office premises where other parameters are fixed, like number of people, working hours, lighting, usage of appliances etc. The cooling loads were simulated hourly and saved in an output file. This file was used for simulating the load component in the TRNSYS model of solar absorption cycle.

Solar based absorption cycle was simulated using TRNSYS. Inputs to collector model was provided from datasheet of SunTrac27, whereas the inputs to absorption chiller model were

provided from datasheet of YAZAKI SC20. There were three control thermostats using in the system, one in collector loop and two in hot water loop of the cycle. They served the purpose of controlling flow rate through collector, control signal of auxiliary heater, and diverting flow from hot water outlet of chiller.

Key parameters were selected to be optimized, based on their importance in the system and availability of time for this study. They were collector area, collector slope, and storage tank volume. Based on parametric analysis and life cycle savings analysis, the optimized values of these key parameters were calculated for selected cities. The results obtained the analysis of simulated solar based absorption system, indicated that with an area of 360 m2 of evacuated tube collectors with an inclination of 12.7° and 10 m3 of storage tank is the optimum configuration of the key parameters for the city of Chennai, maximizing the gain of useful energy of the system and minimizing the consumption of auxiliary energy. Similarly the optimum configurations were also calculated for the other selected cities.

Future optimization studies on solar based absorption system could also be conducted on different control strategies which could be implemented in this system. Control strategies could be put in place in the cooling water loop to vary the cooling water circulation based on the input load at absorption chiller. Another area of future study could be the environmental impact of a solar based absorption system, quantifying the positive impact in terms of CO2 reduction.

List of Figures

Figure 1.1 Generic schemes of physical methods to use solar energy for air conditioning 2

Figure 1.2 Simplified schematic of a solar absorption cooling system 3

Figure 1.3 Types of solar collectors. 5

Figure 1.4 Compression cycle and absorption cycle. 7

Figure 1.3.1 Solar resource availability for India. 13

Figure 1.3.2 Different climatic zones of India. 13

Figure 1.3.3 Efficiency curves of a range of ETC collectors. 14

Figure 1.4.1 Graphical representation of azimuth and altitude angle. 15

Figure 2.1.1 Google Sketchup model representing the simulated building. 18

Figure 2.2.2: TRNBuild model used for calculating cooling load. 19

Figure 2.3.1 Defining schedule type – Workday. 22

Figure 2.4.1 Office temperature, ambient temperature and cooling load at basic configuration. .24

Figure 2.4.2 Heat gain from infiltration, ventilation, internal, total latent at basic configuration. .24

Figure 2.4.3 Office temperature, ambient temperature and cooling load with infiltration OFF.. . 25

Figure 2.4.4 Heat gain from infiltration, ventilation, internal, total latent with infiltration OFF.. . 25

Figure 2.4.5 Office temperature, ambient temperature and cooling load with ventilation ON . . .26

Figure 2.4.6 Heat gain from infiltration, ventilation, internal, total latent with ventilation ON. . 26

Figure 2.4.7 Office temperature, ambient temperature and cooling load when gains are reduced. 27

Figure 2.4.8 Heat gain from infiltration, ventilation, internal, total latent when gains are reduced 27

Figure 2.5.1 Monthly average daily cooling load of selected cities. 28

Figure 2.5.2 Monthly average ambient temperature for selected cities. 29

Figure 3.1 TRNSYS scheme of a solar based absorption cycle. 30

Figure 3.6.1 Hourly cooling load profile for Bangalore. 35

Figure 3.8.1 Solar and auxiliary energy curves with T_collector_out in condition 37

Figure 3.8.2 Solar and auxiliary energy curves with T_toplayer_tank in condition 38

Figure 3.8.3 Variation in monthly solar fraction with changing auxiliary heater temperature. . .. 39

Figure 3.8.4: Hot water loop of simulated cycle with chiller return temperature. 40

Figure 3.8.5 Annual solar fraction over cycle simulation without chiller return thermostat. 41

Figure 3.8.6 Annual solar fraction over cycle simulation with chiller return thermostat. 41

Figure 4.1.1 Monthly average of daily incident solar irradiation for the selected cities. 45

Figure 4.1.2 Annual solar fraction Vs Collector area. 47

Figure 4.1.3 Annual useful solar power Vs Collector area. 47

Figure 4.1.4 Annual heater power required Vs Collector area. 48

Figure 4.1.5 Annual solar fraction Vs Collector area with AHT as 70 °C. 49

Figure 4.1.6 Annual solar fraction Vs Collector area with AHT as 85 °C. 49

Figure 4.1.7 Zoomed in view of annual solar fraction Vs Collector area with AHT as 70 °C . . . 50

Figure 4.1.8 Zoomed in view of annual solar fraction Vs Collector area with AHT as 85 °C. . .50

Figure 4.1.9 Annual auxiliary power required Vs Collector slope for New Delhi. 51

Figure 4.1.10 Annual auxiliary power required Vs Collector slope for Chennai. 52

Figure 4.1.11 Annual heater power required Vs Storage tank volume for selected cities. 53

Figure 4.1.12 Annual useful solar power required Vs Storage tank volume for selected cities. . 54

Figure 4.1.13 Annual solar fraction Vs Storage tank volume for selected cities. 54

Figure 4.1.14 Annual useful solar power required Vs Storage tank volume for different collector areas. 55

Figure 4.1.12 Annual solar fraction Vs Storage tank volume for different collector areas 55

Figure 4.2.1 LCS Vs Collector area with VAM cost as 14 Lakhs. 60

Figure 4.2.2 LCS Vs Collector area with VAM cost as 4 Lakhs. 60

List of Tables

Table 1.1.1 Collector types based on concentration levels and respective efficiencies 4

Table 1.2 Performance parameters of single effect chiller running on different working pair 8

Table 1.3.1 ETC collectors compared for the selection of a study collector. 14

Table 1.4.1 Results of the CA_{max} calculations for selected cities. 17

Table 2.2.1 Heat gain from people 20

Table 2.4.1 Basic configuration of the Load Model. 23

Table 3.1.1 Input parameters for collector Model. 32

Table 3.3.1 Parameters for YAZAKI 20 ton chiller. 32

Table 3.4.1 Flow rates through pumps in system. 34

Table 4.1 Values of parameters in initial simulation for Bangalore. 43

Table 4.1.2 Optimized collector slope for selected cities. 52

Table 4.2.1 Terms used in LCS analysis, their values, unit, and sources. 59

Table 4.2.2 Optimum values of collector area and storage tank volume for selected cities. 61

Table 5.1 Optimum configuration of key parameters for selected cities. 62

Table of Contents

Acknowledgements

Executive Summary

List of Figures

List of Tables

Table of contents

1. Introduction 1
    1.1 Background 2
        1.1.1 Solar Collectors. 4
        1.1.2 Absorption Cycle 6
    1.2 Past studies on solar absorption cooling 8
    1.3 Present Work. 12
    1.4 Collector Spacing. 15
2. Cooling Load Calculation. 18
    2.1 Building Description. 18
    2.2 Load Calculation. 18
        2.2.1 Internal heat gain. 20
        2.2.2 External heat gain. 21
        2.2.3 Thermal comfort. 21
    2.3 Simulation Conditions. 22
    2.4 Parametric Analysis. 23
    2.5 Final Cooling Load. 28
3. System Modeling. 30
    3.1 Solar Collector. 31
    3.2 Storage Tank. 32
    3.3 Absorption Chiller. 33
    3.4 Pumps. 33
    3.5 Cooling Tower. 34
    3.6 Load. 34

3.7 Forcing function. 35
3.8 Control Strategies. 35
4. System Analysis. 43
4.1 Parametric analysis. 45
4.1.1 Collector Area. 46
4.1.2 Collector Slope. 51
4.1.3 Storage tank volume. 52
4.2 Life Cycle Savings analysis. 56
5. Conclusion. 62

Appendix I. 64

Bibliography. 68

1.0 Introduction

While the metropolitan cities of India face severe power shortage, the air conditioners consume a big chunk of the total power demand. This consumption has dramatically increased during the last few decades; this can be attributed mainly to the growing purchasing power and subsequent improvement in living standard in these cities. India, like other developing economies faces a wide gap in the much needed infrastructure to supply the electricity demand. The existing power plant infrastructure supplying electricity to the country relies mainly on fossil fuels. Although currently not under international pressure to reduce its emissions, India will too be forced to reduce its dependency on fossil fuels. The combustion of these fuels produces key contributors to greenhouse gas emissions. Further, the usage of CFCs in air conditioners affects the environment by depletion of the ozone layer. Therefore, a desire to change to more environmentally friendly refrigerants is a motivation in space cooling / air conditioning. So the search is on for a renewable and cheaper source of energy which would not only work as input to comfort cooling but several other energy intensive processes.

The use of solar energy for building cooling, can address the above mentioned environmental and economic problems. Providing comfort cooling using solar energy can be achieved using various technological processes. The term “solar cooling” has been coined to mean the comfort cooling using solar energy. Cooling in a space is generally speaking, trying to remove the heat gain within the spaces from living beings, from electrical appliances; and from heat ingress from the hotter outside ambient and from solar energy streaming in through windows and fenestrations. Therefore, cooling demand is higher in the summers and hotter seasons when there is more solar energy available. This coupling of demand for comfort cooling to higher solar radiation availability makes it a good fit for solar applications. There are many different ways to convert solar energy into cooling or in air-conditioning processes. Such processes are broadly either: Thermally driven or electrically operated. Thermally driven cycles include Absorption cycles, Adsorption cycles and thermo-mechanical processes. The most common electrically driven cooling is derived from the vapor compression cycle. Electrical energy to drive this cycle can be derived from photovoltaic panels.

1.1 Background

The history of solar cooling dates way back to 1878, when the first demonstration of a solar-assisted absorption cooling machine was made during the Paris World Exhibition (Henning, 2007). In 1945 the company Carrier Corp, USA, developed and introduced the first large commercial single-effect absorption cooling machine (ACM) using water/lithium bromine with a cooling power of 523kW, whereas the first commercial double-effect absorption cooling machine (ACM) was manufactured in 1964 by Kawasaki Heavy Industry Co (Eicker, 2009).

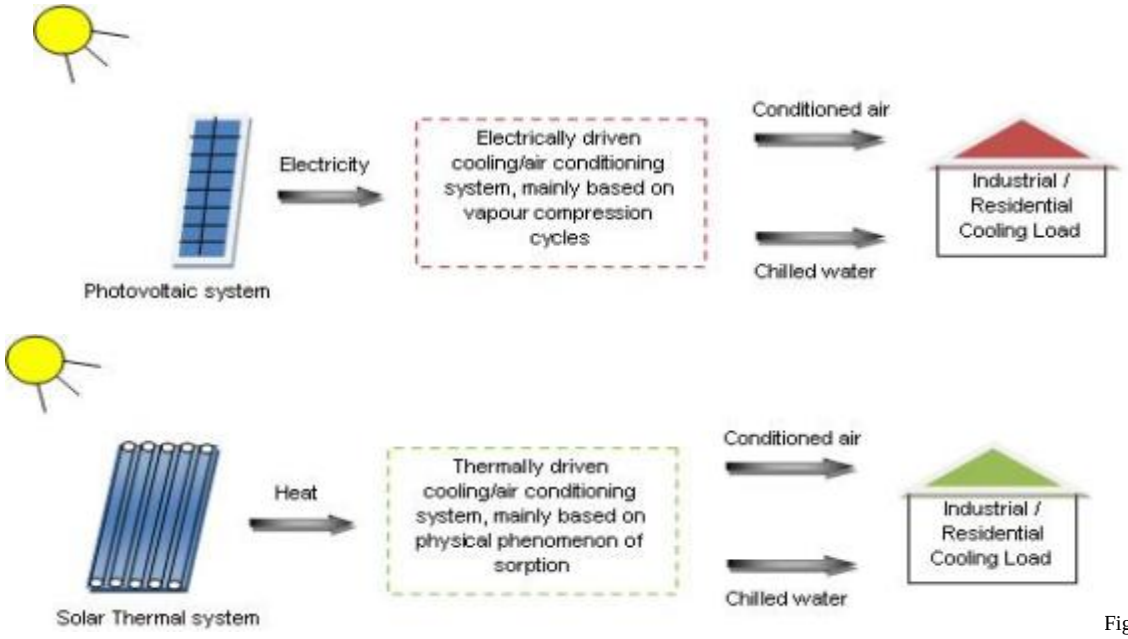

Figure 1.1 Generic schemes of physical methods to use solar energy for air conditioning

Solar energy can be converted into cooling or air-conditioning either by using vapour compression cycles or based on reversible thermo-chemical reactions. The former process requires electricity as an input which can be supplied by photovoltaic panels, whereas the latter's requirement is heat, which can be supplied by thermal collectors. Generic schemes for the conversion process of solar energy in to air conditioning as a product are depicted in Figure 1.1.

Sargon et.al (Sargon, 2011) compares photovoltaic driven compression cycle with thermal collectors driven absorption cycle in his study. He concludes that although the Coefficient of

Performance (COP) of a compression cycle is higher than absorption cycle, Solar Cooling Efficiency (SCE) which is product of radiation collection efficiency and cooling efficiency tends to be higher for the collector based absorption cycle. SCE of a solar absorption cycle is 85%, whereas for solar compression cycle is approximately 75%.

A conventional solar absorption cooling system comprises of solar collectors, a storage tank, an auxiliary heater and the absorption chiller. Fig 1.2 depicts simplified schematic of a solar absorption cooling system. Pumps and thermostats used in the simulated system are ignored during this schematic to make it simpler. Solar collectors are used to convert solar energy into heat, in the form of heating a fluid circulated through it. Storage tank and auxiliary heater are optional components to increase the system performance and reliability, since solar energy is an intermittent resource. Absorption chillers are driven by the heat stored in hot fluid and generate cooling, usually in the form of chilled water. Chilled water produces the desired cooling effect in the conditioned space by lowering the temperature of the indoor air through a heat exchanger.

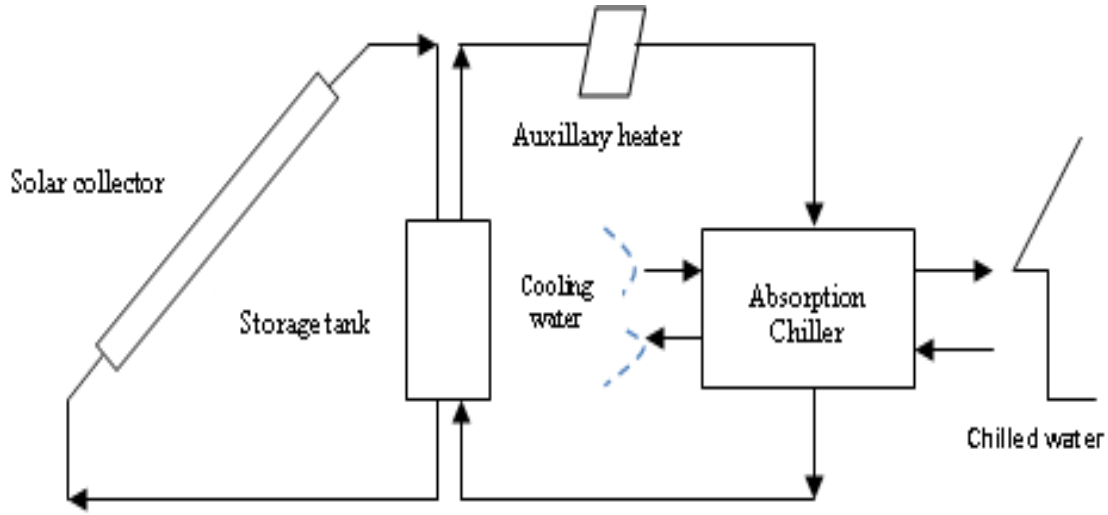

Figure 2.2Simplified schematic of a solar absorption cooling system

1.1.1 Solar Collectors

A solar collector is a device which captures the radiant solar energy and converts it to useful thermal energy. Current solar collectors can beclassified in many ways. One method is according to the optical concentration of the incident radiation – collectors can be classified as non-concentrating, low concentration, medium concentration and high concentration. Non concentrating collectors such as flat plate collectors or evacuated tube collectors do not have optics so that energy incident on their absorbers is at the same intensity as it arrives from the sun. The output temperature from the collector depends on the degree of optical concentration in the design and hence is an important parameter while selecting a type of collector for a specific application. Possible achievable concentration levels and efficiencies of types of solar collectors can be seen in Table 1.1 (Jesko, 2008).

Category	Example	Temperature range, °C	Efficiency, %
No concentration	Flat-plate Evacuated tube	up to 75 up to 200	30-50
Medium concentration	Parabolic cylinder	150-500	50-70
High concentration	Parabodial	1500 and more	60-75

Table 1.1.1 Collector types based on concentration levels and respective efficiencies

The solar radiation that fills our sky can be direct, diffuse or reflected radiation. Direct radiation is also sometimes called beam radiation or direct beam radiation. It is used todescribe solar radiation traveling on a straight line from the sun down to the surface of the earth. Diffuse radiation, on the other hand, describes the sunlight that has been scattered by molecules and particles in the atmosphere but that has still made it down to the surface of the earth. Direct radiation has a definite direction but diffuse radiation is just going any which way. Because when the radiation is direct, the rays are all traveling in the same direction, an object can block them all at once. This is why shadows are only produced when direct radiation is blocked.

Non-concentration type collectors use both direct and diffuse solar irradiation incident on their surfaces, while the concentration type collectors mostly use specular optics and hence can only use the direct solar irradiation as the reflectors are unable to focus diffuse irradiation from various directions on its focal line. The crucial advantage of concentrating collectors is that with a relatively small absorption area they can heat the heat transfer medium to much higher temperatures when compared with their counterparts. Non-concentrating type collectors are normally used in applications that require only low temperatures, less than 100 °C, which makes these ideal for solar cooling applications.

Construction of concentrating and non-concentrating types of collectors can be further understood from Figure 1.3. As seen in the figure, absorbers, heat transfer mediums, and insulation are common elements of collectors, be it concentrating or non-concentrating. Flat plate collectors do contain air between absorber and cover, which results in convective heat loss, whereas this is avoided in Evacuated Tube Collector (ETC) by creating vacuum between absorber and cover glass tube.

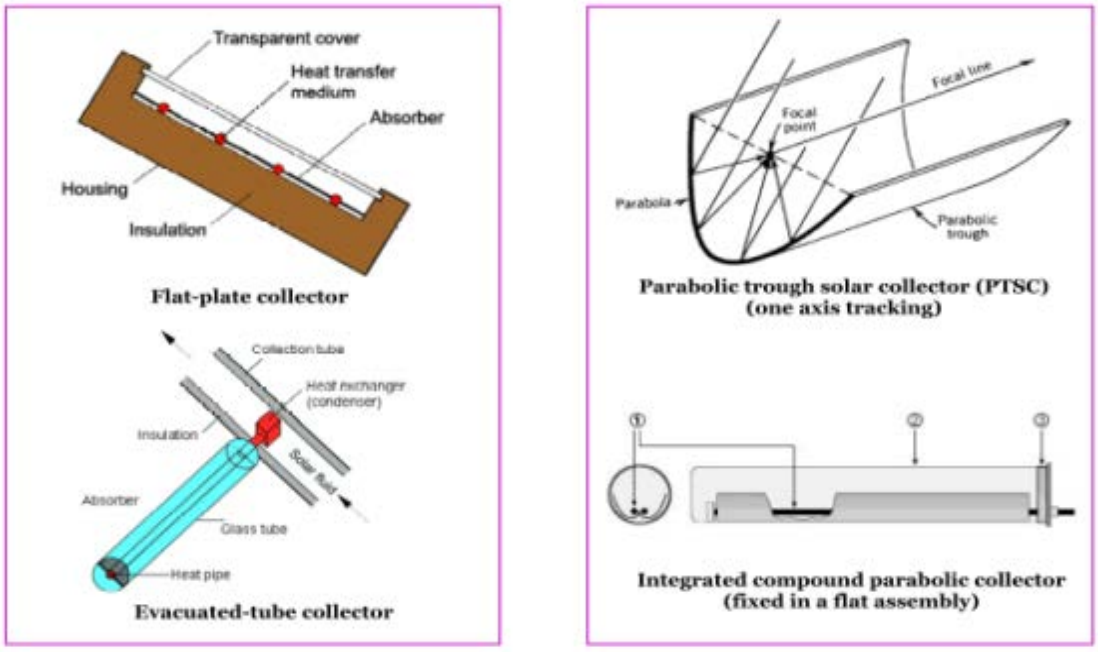

Figure 1.3: Types of solar collectors (Ahmed, 2005)

1.1.2 Absorption Cycle

Absorption cooling machines can be heat driven by utilization of waste heat from different sources, gases exhausted from engines, discarded heat from power plants, and incident radiation from sun input. Environmental friendly absorption cycles do not employ the use of harmful refrigerants and can potentially reduce the peak electricity demand during summers. To figuratively elaborate on the working of absorption cycle and vividly explain the differences between absorption cycle and electrically driven vapor compression cycle refer Figure 1.4.

Compressor is an integral part of the vapor compression cycle, whereas the absorption cycle uses fluid pump which requires less energy and is cheaper to operate, for producing the required pressure difference. A vapor compression cycle which requires electricity as an input compresses the refrigerant to a relatively high pressure using a compressor and then condenses it by rejecting the heat to ambient conditions in the condenser part. The refrigerant then flows into the expansion valve and then to an evaporator, which is a relatively lower pressure with a combination of vapor and liquid states of the refrigerant. The liquid form of the refrigerant after absorbing heat from the water to be chilled then vaporizes into the vapor state. This process thermally produces the desired cooling effect in a vapor compression cycle.

In an absorption cycle, the required effect of compressing the refrigerant is produced by raising the pressure of water vapor by absorbing vapor at low pressure in absorber and consequently desorbing this vapor at a high pressure in the regenerator (Qu, Ming 2008). The produced water vapor is then absorbed at a lower pressure by the concentrated sorbent solution in the absorber. Then a solution pump pumps the diluted solution to a higher pressure and temperature in the regenerator. By addition of thermal energy to the sorbent solution in diluted form, the water vapor is separated and then condensed after having rejected its heat to the cooling water in the condenser. The rest of the processes in the absorption cycle i.e. removal of heat from chilled water in evaporator and vaporization of the water refrigerant are similar to the ones in compression cycle.

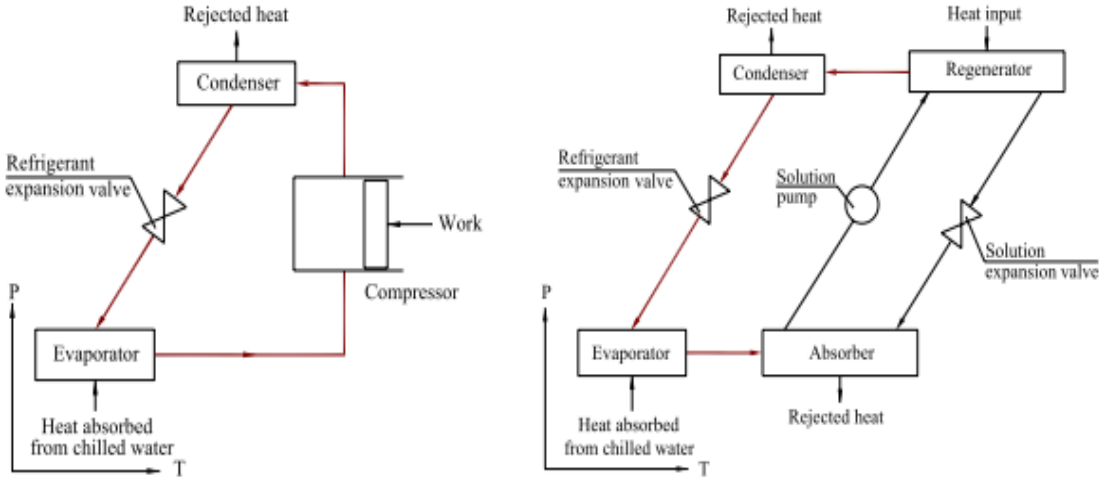

Compression Cycle **Absorption Cycle**

Figure 1.4: Compression cycle and Absorption cycle (Qu, Ming, 2008)

Absorption chillers are categorized either by the number of effects or by the number of lifts. Effects refer to the number of times high temperature input heat is used by the the absorption machine, increasing the number of effects is meant to increase the COP using higher driving temperature levels. Whereas the lifts refer to the number of generator/absorber pairs to successively increase the refrigerant concentration in the solution and to thus reduce the required heat input temperature level (Eicker, 2009).

Most commonly working pairs of fluids in absorption chillers are water/lithium bromide and water/ammonia. Latter pair can produce cold temperature as low as -50 °C, whereas water/lithium bromide pair cannot produce a cold temperature of lower than 6 °C. It can be seen from Table 1.2, that the required heat input temperature for water/ammonia pair is also much higher than water/lithium bromide pair. Although the COP for both pairs is in the same range, the major difference lies in the range of cold temperature it can produce, which makes both unique for different kind of applications.

	Water/LithiumBromide	**Water/Ammonia**
cold temperature, °C	6 to 20	-30 to 20
heating temperature, °C	70 to 110	90 to 160

cooling water temperature, °C	30 to 35	30 to 50
COP	0.5 to 0.7	0.4 to 0.6

Table 1.2: Performance parameters of single effect chiller running on different working pair

1.2 Past studies on solar absorption cooling

There has been extensive research on solar cooling date, both experimental and simulation based. Roughly more than 100 solar based air-conditioning systems are currently installed in Europe (K4RES-H, 2006) alone. The usage of these systems can save 30% to 60% of electricity required for air-conditioners, but due to several constraints these potentials are often not yet realized in the installed systems. Balaras et al. (2007) cited that a total of 54 solar air-conditioning projects in Europe are in operation, 33 of them are working with lithium bromide-water absorption chillers. Single-effect lithium bromide-water (LiBr-H2O) chiller, the most popular machine in solar cooling dude to its low temperature operability, has been incorporated in numerous studies including the following demonstration and pilot projects.

Ward and Lof (1975) reported that the first integrated system providing heating and cooling to a building by use of solar energy had been designed and installed in a residential-type building at Colorado State University. Solar heated liquid supplied heat both air circulating in the building and lithium bromide absorption air conditioner. They reported that approximately two-thirds of the heating and cooling loads are expected to be met by solar energy. Ward et al. (1976) cited for the Solar House I, solar heating and cooling system became operational on July 1, 1974. From August 1, 1974 to January 13, 1975, approximately 40% of the cooling load was provided by solar energy.

Furthermore, Ward et al. (1978) reported that the use of cool storage in conjunction with residential lithium bromide absorption chillers allows improved operating conditions of the cooling subsystem and significantly improves the seasonal average coefficient of performance of the cooling system. Perez (2007) reported that (Sayigh and Saada, 1981) had installed a 12.31 kW cooling solar-driven absorption chiller in Riyadh, Saudi Arabia. The

system included flat collectors with a total area of 56m^2, a hot water storage tank with a volume of 24m^3 that was able to operate the system for 15h at chilled water outlet temperatures of 17 °C.

Hattem and Dato (1981) installed a solar absorption cooling system in Ispra, Italy, which consisted of a 4kW chiller and 36m2 flat plate collectors and two hot water storage devices of 0.3 and 2m^3. They reported that the chiller coefficient of performance (COP) and the overall system efficiency were 0.54% and 11%, respectively. Bong et al. (1987) designed, installed and operated a solar powered 7kW absorption chiller in Singapore. The system included heat pipe collectors with a total area of 32m^2, an auxiliary heater, a hot water storage tank, and a 17.5kW cooling tower. They reported that the overall average cooling capacity provided was 4 kW, COP of 0.58 and a solar heating fraction of 39%. The fraction of the total driving heat load, which is covered by solar energy, is referred to as solar heat fraction.

Al-Karaghouli et al. (1991) reported the operation results of a solar cooling system installed at the Solar Energy Center in Iraq, which was considered to be the largest solar cooling system at the time. The system was equipped with two absorption chillers of 211.02 kW cooling each, 1577 evacuated tube collectors and two thermal storage tanks of 15m^3, five cooling towers with various backup systems. They reported that the daily average solar collection efficiency is 49%, chiller COP of 0.618 and solar heating fraction of 0.604. Yeung et al. (1992) designed, constructed and implemented a solar-driven absorption chiller of 4.7 kW nominal cooling capacity at the University of Hong Kong. The system included flat collectors with a total area of 38.2m^2, a 2.75m^3 hot water storage tank, a cooling tower and other auxiliary equipment. They reported that the collector efficiency was estimated at 37.5%, the annual system efficiency at 7.8% and an average solar fraction at 55%, respectively.

Meza et al. (1998) reported the performance parameters of an experimental pilot solar assisted system installed in Cabo Rojo, Puerto Rico, that consisted of a 35.17kW cooling absorption chiller, powered by 113m2 of selective surface flat plate collectors, a 5.7m^3 hot water storage tank, a 84 kW cooling tower and other auxiliary equipment. The overall absorption system collector array efficiency was 30.5%, the nominal cooling capacity was measured at 25kW with a COP of 0.63% and a 95% solar heating fraction.

Best and Ortega (1999) summarized the results of a solar cooling project from 1983 to 1986 in Mexico. The system include 316m^2 flat plate collectors, 30m^3 heat storage tanks, a maximum capacity of 90 kW LiBr-H2O absorption chiller and a maximum capacity of 200kW cooling tower. Their system after modification improved the yearly solar heating fraction increased from 59% to 75% and the chiller efficiency varied from 0.53 and 0.73 when hot water was provided at temperatures between 75 and 95 °C at coolant water temperatures of 29-32 °C and chilled water temperatures of 8-10 °C, respectively. Li and Sumathy (2001) presented the results of a solar powered air-conditioning system with a partitioned hot water storage tank. The system employs a flat-plate collector array with a surface area of 38m^2, a LiBr-H2O absorption chiller of 4.7 kW cooling capacity and a two partitioned hot water storage tank of 2.75m^3.

Syed et al. (2005) reported the performance of a LiBr-H2O absorption chiller with 35.17 kW cooling nominal cooling capacity driven by hot water from 49.9m^2 flat plate collectors with 2m^3 hot water storage tank installed at a typical Spanish house in Madrid. Since the solar system was originally designed for 10 kW cooling capacity, the absorption chiller yielded the maximum cooling capacity of only 7.5 kW and daily and period average COP were 0.42 and 0.34, respectively. Kim (2007) cited that (Storkenmaier et al., 2003) reported the development of a 10kW water-cooled absorption chiller. The machine is capable of producing chilled water at 15°C when the driven hot water is at 85 °C, being cooled by cooling water at 27 °C with the COP of 0.74. The cooling capacity varied between 40% and 160% of the nominal capacity with the hot water temperature increasing from 56 to 105 °C.

Furthermore, Kim (2007) cited that Safarik et al. (2005) presented the performance data of a water cooled absorption chiller. The machine produced about 16 kW cooling water at 32°C with COP of 0.75. Zambrano et al. (2007) presented results of a solar absorption cooling plant which has 35.17 kW cooling nominal cooling capacity at Seville in Spain. The plant has flat plate collectors with a total area of 151m^2, a 2.5m^3 hot water storage tank and an auxiliary gas heating system. They tabulated the instantaneous values of the solar, gas power supplied to the generator, and the chiller cooling capacity for one day running in May only, no information was cited about the long-run performance. Pongtornkulpanich et al. (2007) designed and installed a 25.17 cooling solar driven absorption cooling system in Thailand in

2005. The system has a 0.4 m^3 hot water storage tank and 72 m^2 evacuated tube solar collectors that delivered a yearly average solar heating fraction of 81%.

Since setting up a system is both time consuming and expensive, computer modeling of thermal systems does present numerous advantages. Some of the most important advantages are elimination of the expense of building prototypes, optimization of the system components, estimation of energy delivered from the system, and prediction of temperature variations of the system (Assizadeh, 2004). On 6th July, 2011, Thermax India Ltd, claimed to be the first in the world to have commissioned a 100kW solar cooling system at the Solar Energy Center in Gurgaon, Haryana. The project integrated a triple effect chiller with solar parabolic concentrators. Although the technical details of the project are yet undisclosed, the project shows the arrival of solar cooling in the country.

Florides (Florides, 2002) modeled and simulated an absorption based solar cooling system using TRNSYS for Nicosia, Cyprus and concluded with an optimized system configuration of 15-m^2compound parabolic collector, tilted at 30 Degree and a 600 litre storage tank. The author considered nonsubsidized fuel cost for the life cycle savings, as the then subsidized costs would've given an even lower savings, although the system was was still economically unfeasible. Whereas Ghaddar et al. (Ghaddar, 1997) modeled and simulated a solar absorption system for Beirut. The results suggested that a minimum collector area of 23.3 m^2 is required for a ton of refrigeration, which does not fall under the range proposed by Eicker (Eicker, 2009) of less than 8m^2. Hence, it was observed that the optimization results vary immensely from location to location.

In 2005, a 10-ton $LiBr/H_20$ based single effect absorption cooling system became fully operational at the School of Renewable Energy Technology (SERT), Phitsanulok, Thailand. Pongtornkulpanich et al. (Pongtornkulpanich, 2007) reported that an array of 72m^2 of evacuated tube solar collector was able to produce an annual solar fraction of 0.81, while the rest 19% had to be supplied by the auxillary heater. The author concludes by pointing out that although the system is not economically attractive, it might serve as a proof of concept.

Zambrano et al (Zambrano, 2007) presented results of a solar absorption system of 35 kW cooling capacity, installed in the city of Seville (Spain). This installation consists of 151 m^2 of

flat plate collectors, a storage tank of 2.5 m^3 and an auxiliary gas heating system. Ahmed et al (Ahmed, 2007), presented the performance evaluation of real integrated installation of refrigeration. This facility has been in operation since 2002, in Oberhausen, Germany. The space included a floor of 270m^2, for which the system was designed with an absorption chiller Lithium Bromide-Water with 35 kW capacity, 108m^2 of collector area of evacuated tube collectors inclined at 32 Degrees and storage tanks of 6.8m^3 for hot water and 1.5 for cold water.

With respect to the advancement in the field of simulation study of solar cooling, Vidal et al (Vidal, 2009) states that one of the recommendations to bring down one of the main barriers to the penetration of solar absorption refrigeration in the market (the high initial cost) is to develop new models and tools for dynamic simulation of these systems, which will allow to do an optimum sizing of the system, long term performance studies and economic feasibility analysis of projects.

1.3 Present Work

This study is aimed at optimizing the solar based absorption cycle using the simulation of the same. It investigates the technical and financial aspects of an optimized solar thermal based single effect absorption cycle model for Indian conditions. Four cities were selected for the purpose of analysis. Since India is a large country with different climatic zones, one city was picked from each climatic zone. Figure 1.3.1shows the different climatic zones in India with selected cities. Figure 1.3.2shows the NREL produced map of solar resource availability across India. This variance will be useful in evaluating the feasibility of the system for different weather conditions. The cities selected for the analyses are from henceforth in the thesis are cited as “selected cities”.

Considering the above criteria in mind, the following cities are selected:

1. Jodhpur (DNI: 5.5- 6.0 kWh/m2/day , Zone: Hot and Dry)
2. New Delhi (DNI: 4.0-4.5 kWh/m2/day , Zone: Composite)
3. Bangalore (DNI: 5.0-5.5 kWh/m2/day , Zone: Temperate)
4. Chennai (DNI: 4.5-5.0 kWh/m2/day , Zone : Warm and Humid)

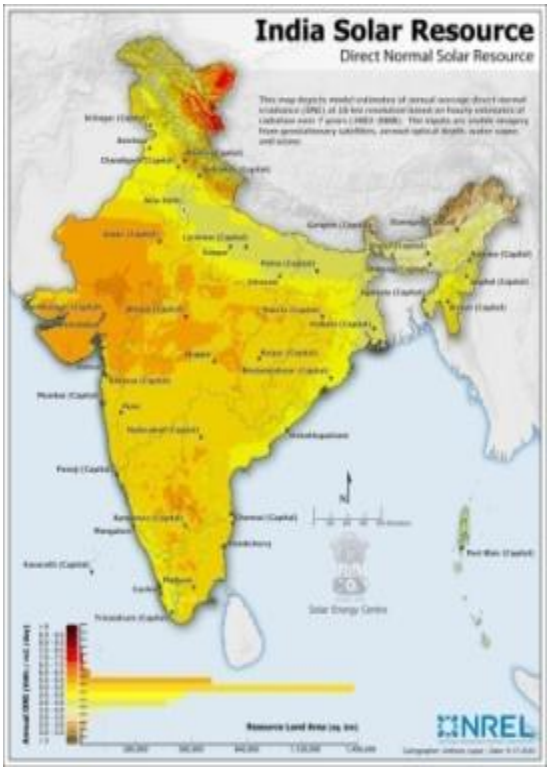

Figure 1.3.1 Solar resource availability for India (NREL, 2010)

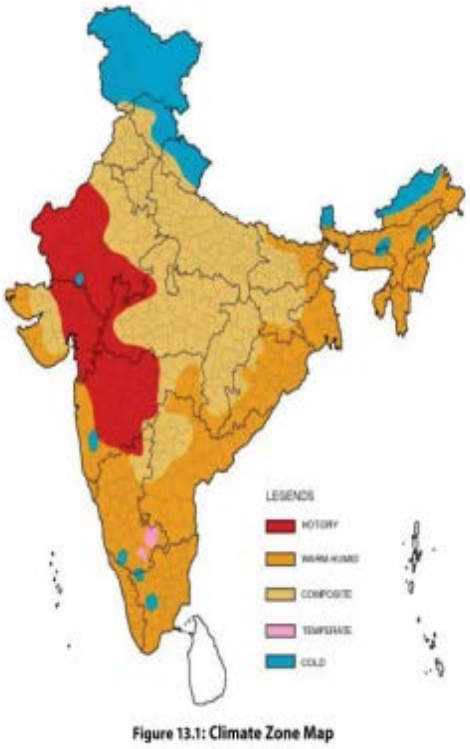

Figure 1.3.2: Different climatic zones of India (MNRE, 2012)

Evacuated Tube type solar Collector (ETC) was selected for this thesis based on the results from Assilzadeh (Assilzadeh, 2005) and Florides (Florides, 2002) The higher efficiency and comparatively not so high cost made it the choice for this study. ETCs are pretty common in the Indian market, primarily being used for the purpose of water heating. SRCC is an organization conducting performance tests for commercial collectors, the results from which are widely accepted. The datasheets of the list of collectors mentioned in Table 1.3.1 were referred to for their efficiency parameters. The particular ETC to be used in this study was then selected after going through the efficiency curves of these collectors, these curves can be seen in Figure 1.2.3. The selected collector is Energistic Suntrac27 because of the higher performance of the product over the entire range of input temperatures to the collector.

CollectorType	Company	Collector Name
ETC	Apricus	AP-30C
ETC	Energistic	SunTrac27
ETC	Jiangsu Sunrain	TZ58/1800-25R2
ETC	KingspanThermomax	DF100-10
ETC	Oventrop	OV 5-24 AS/AB
ETC	ergSol	erSol 202 df

ETC	SolarUs	SL-30
ETC	EarthNet	ENE24

Table 1.3.1: ETC collectors compared for the selection of a study collector

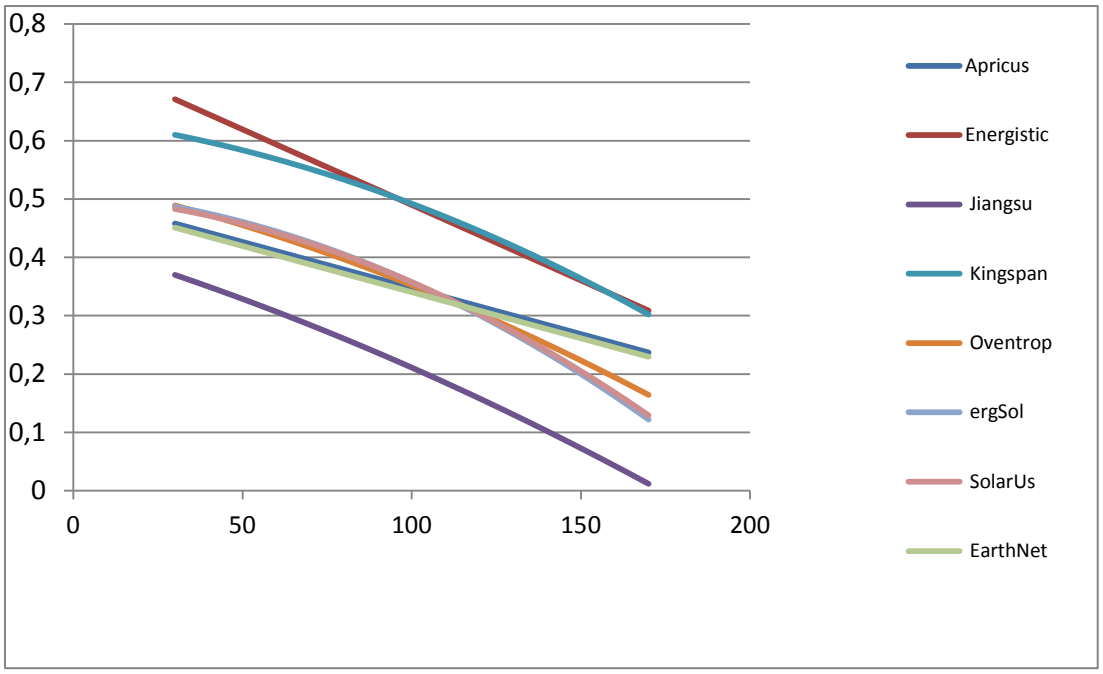

Figure 1.3.3: Efficiency curves of a range of ETC collectors

The chiller model which was selected for this study was absorption based single effect chiller with a capacity of 20 Tons. The datasheet of a chiller of similar characteristics from the company YAZAKI was used for the simulation of the chiller component of the cycle. The choice of size of the VAM was driven by the existing 20 ton system in the Siemens office. The aim was to simulate the cooling load for an office space with similar construction to the offices of the Siemens Corporate Research Center, Bangalore. The area was sized such that the peak cooling load in the space would not exceed 20 tons in any of the climatic zones. The office space area selected was 1250 m^2in order to meet these considerations. The upper limit of the collector area which can be used in the system is defined by how many collectors can be placed in the given space. Hence for this simulation the maximum Collector Area (CA_{max}) which can be accommodated in the given space of 1250 m^2 was calculated. This exercise was repeated for each of the selected cities.

1.4 Collector Spacing

Avoiding shading is very crucial while designing a solar array. The net sun-hours for any location in India would be in the range of 5 to 9 hours, depending on the region it belongs to. Hence, any obstruction to the sunlight should be avoided. In the case of photovoltaic devices, shading a single corner of the module can drastically reduce the production by half, so avoiding shading onto the PV array is of utmost importance. The effect of shading on solar thermal collectors though prominent, is not as significant as in the case of PV arrays. Shading is mainly a concern where the optimum use of space while placing solar collectors or arrays is required be it on ground mounts or some flat roof mounts. With limited solar resource and steep penalties for failure, properly determining correct shade spacing is a critical calculation in solar system design.

The procedure for calculating shadow spacing starts with the sun's position in the sky on the winter solstice, December 21st. As this is the day when we get the lowest solar altitude angles for a particular location i.e minimum solar altitude angle α. Solar altitude angle is the angle the sun makes with the ground in your shade-free solar window.

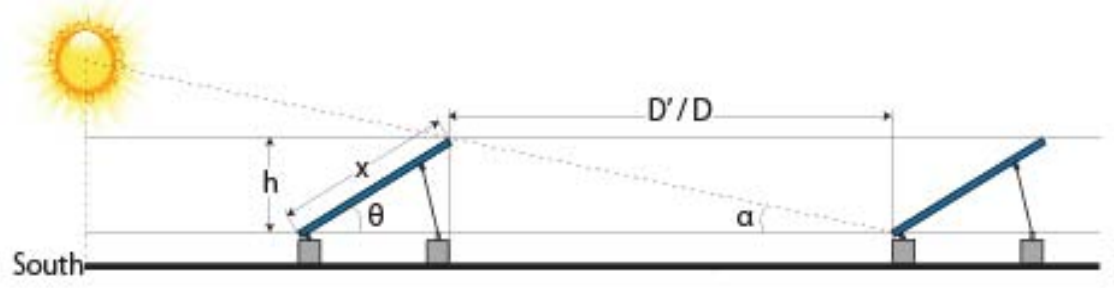

Figure 1.4.1: Graphical representation of azimuth and altitude angles.

The altitude angle depends on the latitude of the location in consideration. For this study these calculations were done for the selected 4 cities in India. Azimuth and altitude angles were calculated for the selected day i.e winter solstice from 7:00am till 5:00pm with an internal of one hour.

The shadow length of the collector depends on the collector length, direction of orientation, azimuth angle and altitude angle. For most ground and roof mounted systems where row spacing is a concern, the height (h) of the obstruction can be directly obtained from the

dimensions of the solar panel and the array tilt. Alternately, it can be measured as the difference in height between the bottom/leading edge of one row and the maximum height of the next row south of it, or a direct measurement of whatever obstruction you want the array to avoid. Using this height, the maximum shadow distance can be obtained. The shadow distance is found through using simple trigonometry. Equation 1.2.1, as shown below is used:

$$D' = h/\tan\alpha \qquad \text{Equation 1.2.1}$$

From here, just one more calculation gives the minimum inter-row spacing needed to avoid shade within your solar window. This is called the "Solar Azimuth Correction". Using the morning sun position, the equation is used to calculate this factor is equation 1.2.2The symbols used in the equations can also be graphically understood from Figure 1.2.4.

$$D = D' * \cos(180 - \psi) \qquad \text{Equation 1.2.2}$$

Where:

T = Time period for array to be shade-free on winter solstice, typically 4-6 hours

α = solar altitude angle

ψ = solar azimuth angle

h = height of obstruction (where $h = x * \sin(\theta)$ for titled solar arrays)

x = tilted module length

θ=tilt angle

D = Minimum array row spacing

D' = Maximum shadow length

These calculations of row shadow lengths and row spacing were performed for the selected collector, for each selected city separately. The values selected were then used to calculate the number of arrays of the collector which can be accommodated for each city. The results of these calculations were as shown in Table 1.4.1.

City	Shadow Length (m)	Inter-row spacing (m)	CA_{max} (m^2)
Bangalore	0.967	0.579	980

New Delhi	3.346	2.248	640
Jodhpur	3.329	2.084	640
Chennai	0.899	0.588	980

Table 1.4.1: Results of the CA_{max} calculations for selected cities

Once these calculations were done the simulation stage of the thesis was started. Chapter 2 discusses in detail the simulation conditions adopted for the calculation of cooling load for the selected cities, the simulation of the cooling load under the specified conditions and it also analyses the parameters affecting the cooling load and their quantitative impact on the load relative to other parameters. This simulation was performed using TRNBuild.

Chapter 3 elaborates on the simulation of solar absorption cycle using TRNSYS. Beginning with a brief overview of the absorption cycle being simulation along with the simulation conditions, it describes in detail the components of the software used to represent the system components. It analyses the dependence of system performance on key parameters like collector area, collector slope, storage tank size and thermostat settings.

Chapter 4 discusses the results of parametric analysis performed on the simulated system to find the optimized values of key parameters. It also describes the Life Cycle Savings (LCS) analysis used to find the optimum collector area. The results are obtained after several iterations of the simulations for the selected cities, under varying parameters. These results are then discussed in Chapter 5 along with the future research prospects in simulating such systems.

2.0 COOLING LOAD SIMULATION:

To simulate the solar cooling system, one of the crucial requirements is of the cooling load. This load will in turn later be input in the model of the chiller component of the system in TRNSYS. Since the project requires just the cooling load, the calculation of heating load or any other structural calculations were not performed using the simulation. The weather conditions for the selected cities are simulated using Meteonormfiles, a dataset containing climatological data for different locations and time of the year. Since weather data is only available for selected cities in Meteonorm database, this was taken into consideration while selecting the cities.

2.1 BUILDING DESCRIPTION:

TRNBuild was used to simulate an office building floor and the cooling load of this building was considered as the load for Solar Driven Absorption Cycle (SDAC). The building structure simulated in the model is based on observations of the construction of first floor at SIEMENS Corporate Research Center in Bangalore, India. The floor modeled is the first floor of the office complex. Figure 2.1.1, is a Google Sketchup model of the same. The building is a structure which is neither insulated nor shaded, like typical office buildings in Indian cities.

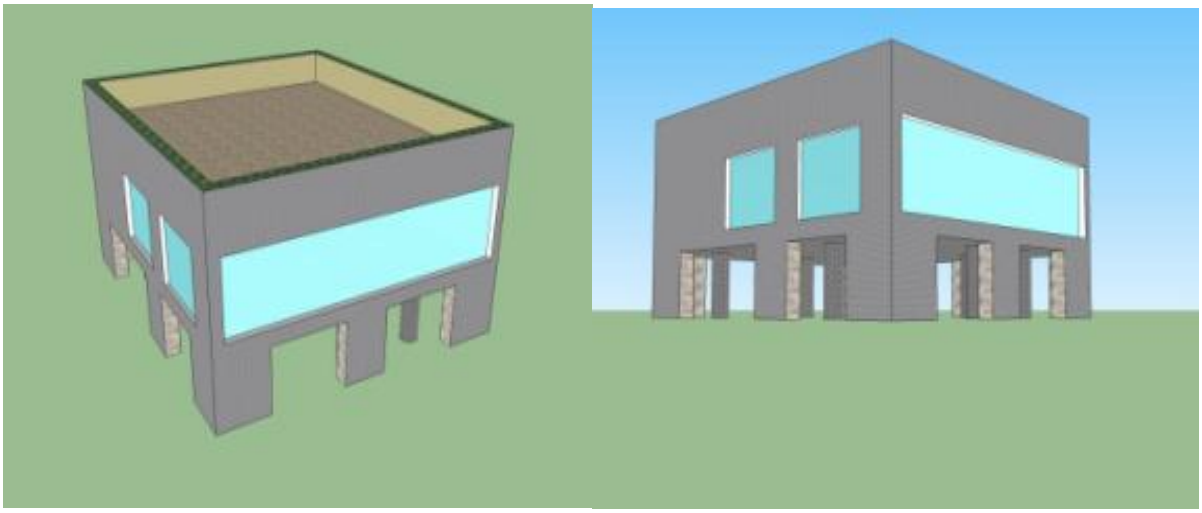

Figure 2.1.1: Google Sketchup model representing the simulated building

2.2 COOLING LOAD CALCULATION

The simulation model made to represent such a building in TRNBuild has different components representing each step of the process of calculating cooling load for a building. The entire scheme of the model is represented in a screenshot of the model i.e. Figure 2.2.1. The intricate model manages various factors such as lighting arrangements, people occupancy routines, ventilation in the system, infiltration in the system, weather conditions, design of the building etc. Simulation may look complicated at first but TRNBuild generates this scheme based on user friendly graphical inputs. The parameters used to simulate the cooling load calculations for this thesis, and their individual effects on the cooling load are discussed in more detail in the following paragraphs.

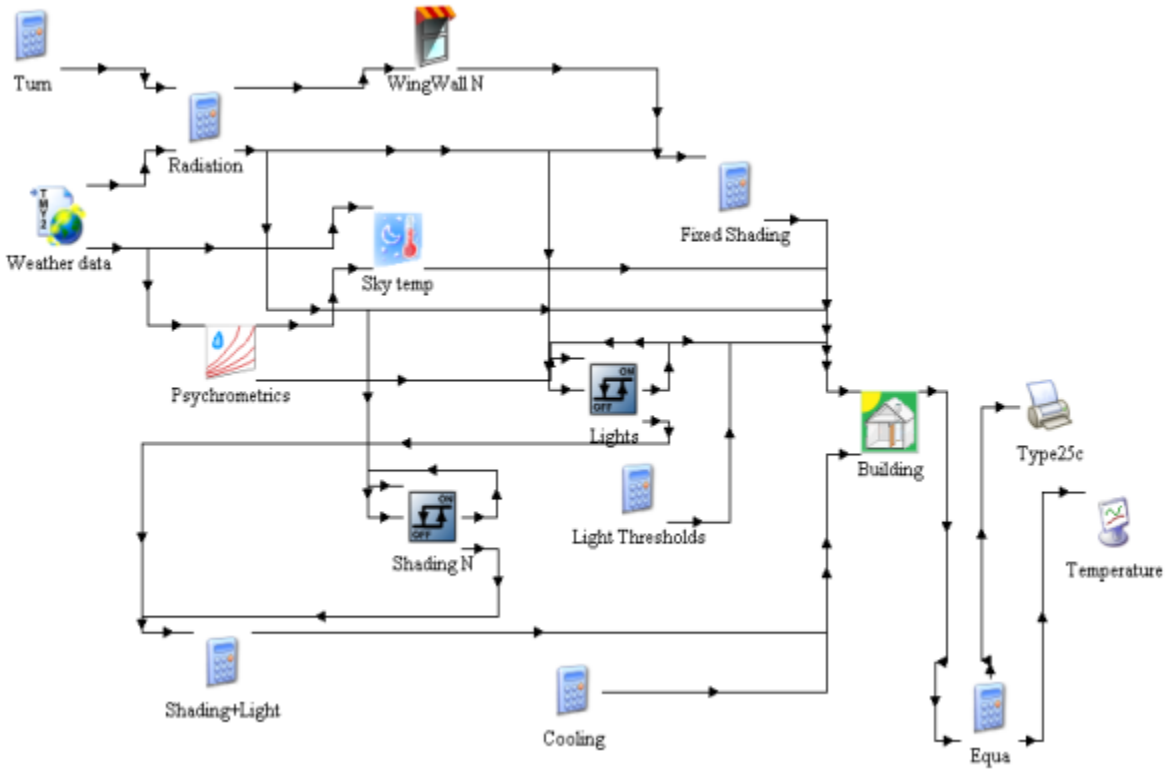

Figure 2.2.2: TRNBuild model used for calculating the cooling load requirement.

What is cooling load? The amount of heat energy to be removed from a building by the use of HVAC equipment to maintain the premises at the design comfort conditions is referred to as cooling load (or heat gain). This cooling load depends on 3 parameters: Internal heat gain, External heat gain, and the thermal comfort conditions. These factors and their impacts on the cooling loads are now discussed.

2.2.1 Internal heat gain

This can be termed as the collection of heat given off by sources (people, electrical equipment etc.) inside the building.

- People: The values for heat gain from occupants of conditioned space selected from the predefined values available in TRNBuild are compared with the standard values for the same conditions as per ASHRAE standards in table 2.2.1. The difference is small and hence has been ignored.

	Degree of Acitivity	Typical Application	Total Heat Adjusted (Watts)	Sensible heat (Watts)	Latent Heat (Watts)
TRNBuild	Seated, light work, typing	Office, Hotels, Apts	150	75	75
ASHRAE*	Seated, light work, typing	Office, Hotels, Apts	140	75	65
	*Source: Table 1 - Chapter 18, ASHRAE Handbook				

Table 2.2.1: Heat gain from people

- Lighting: The lighting power density selected is 13 W/m^2. The value of lighting power density as per ASHRAE standards (Source: Table 2 – Chapter 18, ASHRAE Handbook) are 12 W/m^2 for office space and 14 W/m^2 for Conference rooms. Since the closest available options in TRNBuild are 10 W/m^2 and 13 W/m^2, the latter option is selected being closer to the optimum value.

- Laptops: Each laptop with 50 W heat radiation is selected. As per ASHRAE standards (Source: Table 8 – Chapter 18, ASHRAE Handbook), the value of heat gain for a laptop Model B from Manufacturer A with 2.3 GHz processor and 2GB RAM is 49 Watts.

- Office Equipment: Other office equipment simulated for internal heat gain purposes are an office printer, hot beverage vending machine, water cooler and a microwave. The

heat gains used for the modeling these equipment are as per ASHRAE standards (Source: Table 9/10 – Chapter 18, ASHRAE Handbook).

2.2.2 External heat gain

The incident solar radiation on the windows and rooftop can drastically raise the internal temperature of a building. This process is called external heat gain. Aside from planting trees and changing the color of your house and roof, not much can be done to ward off external heat gain.

- Wall Type: Since all the walls in TRNBuild library are ASHRAE standard walls, the configurations don't need any validation. As the Siemens office building and other buildings in general are not well insulated in India, the walls are considered to be made single element (concrete) without any insulation and with a leaky infiltration i.e. of approximately 0.6 l/hr.
- Orientation: The walls are assumed to be facing the four cardinal directions without any inclination.
- Windows & Shading: The wall facing north is assumed to have approximately 80% of it's area i.e 20 m^2 as a single glass window. Whereas walls facing East and West have around 20% window area i.e 6 m^2 each. Wall facing the south direction doesn't have any window. These are rough estimations approximately of the Siemens Corporate Research office in Bangalore

2.2.3 Thermal Comfort

Thermal comfort is that condition of mind that expresses satisfaction with the thermal environment.

- Metabolic rate: Since the metabolic rate for "filing, seated" person in office environment is 1.2 mets as per the ASHRAE standards (Source: Table 4-Chaper 9, ASHRAE Handbook). This value is considered as an input into the TRNBuild model.
- Clothing Factor: Since model is for an office space, an acceptable assumption is that of trousers, full sleeve shirt, briefs and shoes. For this particular set of clothes the clothing factor is 1.2 as per ASHRAE standards (Source: Table 7-Chapter 9, ASHRAE Handbook).

2.3 SIMULATION CONDITIONS:

The simulation to calculate the cooling demand was performed under a particular set of conditions, which are as follows:

Schedule: Since the building being replicated is that of an office, a working day schedule is used for the calculations. As shown in Fig 2.3.1, the output value is 1 during the typical working hours in Siemens i.e. 08:00 to 19:00 hours and 0 otherwise. People occupancy and the use of electric appliances are also dependent on the value of schedule.

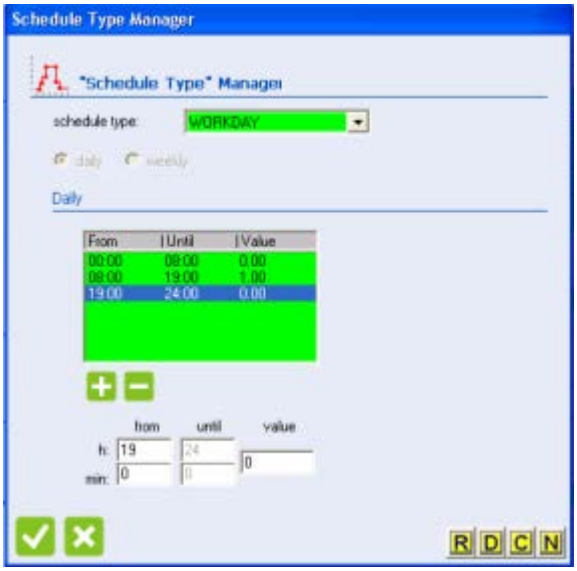

Fig 2.3.1: Defining schedule type - Workday

Ambient Conditions: Climatological conditions of the city of Bangaloreare simulated in TRNSYS using Meteonorm file for the same, since the Siemens Office being modeled is located in this city.

Cooling Conditions: The model maintains an upper limit of 26 DegC as the inside temperature of the designed office space.

2.4 PARAMETRIC ANALYSIS

To study the effect of key parameters on the cooling load, parametric analysis was conducted. The analysis was done for a period of 3 days (72hours) in summers; hence the simulation starts from 4320 hours and ends at 4392 hours. A shorter time period was considered to study the effects more clearly. All the variations were done within this time period. Conditions used to calculate cooling load for this study are termed as basic configuration, these values and conditions have been explained in this chapter. Table 2.4.1 shows the basic configuration used for calculating the cooling load for selected cities.

Basic Configuration	
Floor Area	1250m^2
Infiltration	Leaky (0.6l/hr.)
Ventilation	OFF
Heating	ON
Cooling	ON at 26 °C
No of Persons	70
Gain from a person	14 W
No of Laptops	70
Gain from laptop	50 W
Lighting Gain	13 W/m^2

Table 2.4.1: Basic Configuration of the model

Figure 2.4.1 shows the trend of office temperature (red color plot) and ambient temperature (blue color plot) plotted on the left Y axis, whereas the cooling load of the building (area 1250 m^2) in plotted in pink on the right Y axis. These trends were plotted using basic configuration of the model. Using the same configuration, heat gains from infiltration, ventilation, total convective heat gain, and total latent gain were plotted in Figure 2.4.2. In this plot, red color depicts heat gain from infiltration, blue depicts heat gain from ventilation, orange depicts total convective internal heat gain, and green depicts total latent heat gain from internal components. Since ventilation is switched OFFi.e there isn´t any exchange of air with surroundings in the standard conditions, it

can be seen that heat gain due to ventilation is zero. Or in another words it can be noted in Figure 2.4.2 that there is no blue curve, it is because blue curve represents heat gain from ventilation, which in the standard case is zero. Heat gain through infiltration which is represented by red color curve in the plot, has a low value. It is due to the fact that infiltration rate present in the system is low i.e 0.6 l/hr. This rate of infiltration is also referred to as leaky infiltration.

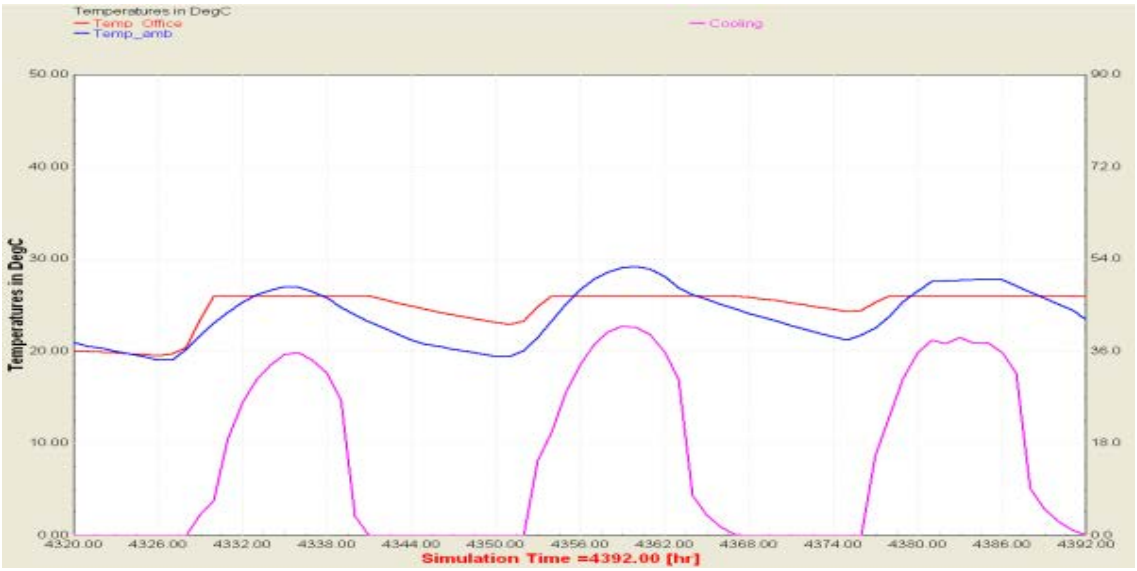

Fig 2.4.1: Office Temp (red) and Ambient Temp (blue) are plotted on the left Y axis in DegC, whereas the cooling load of the building (120m2) is plotted in pink on the right Y axis (kW).

Fig 2.4.2: Heat gains from various internal components. “red” color depicts heat gain from infiltration, “blue” depicts heat gain from ventilation, “orange” depicts total convective internal heat gain, and “green” depicts total latent heat gain from internal components.

Now we shall notice the difference in cooling load by varying each parameter, individually.

- Infiltration: The infiltration value is changed to NO infiltration per hour. It can be seen in Figure 2.4.3 and Figure 2.4.4 that there is minimal change in the cooling load curves (in the order of 0.2-0.6 kW) and the heat gain from infiltration becomes zero, as the infiltration rate was not so high. The cooling load decreases but very slightly.

Fig 2.4.3: Ambient temp, office temp and cooling load curves when infiltration is OFF

Fig 2.4.4: Heat gain curves when infiltration is OFF

- Ventilation: Ventilation rate is changed from 0 air changes per hour to 5 air changes per hour i.e. changed to ON state from previous OFF. Since ventilation takes in ambient air, there is a drastic increase (order of 10-15 kW at peak) in the cooling load as seen in the Figure 2.4.5 below. This can directly be attributed to the heat gain from ventilation as seen in Figure2.4.6 in “blue”. It can also be seen that the increase is only on the days when the ambient temperature increases more than 26 °C, which is the temperature where cooling starts.

Fig 2.4.5: Ambient temp, office temp and cooling load curves when Ventilation is 5ACH

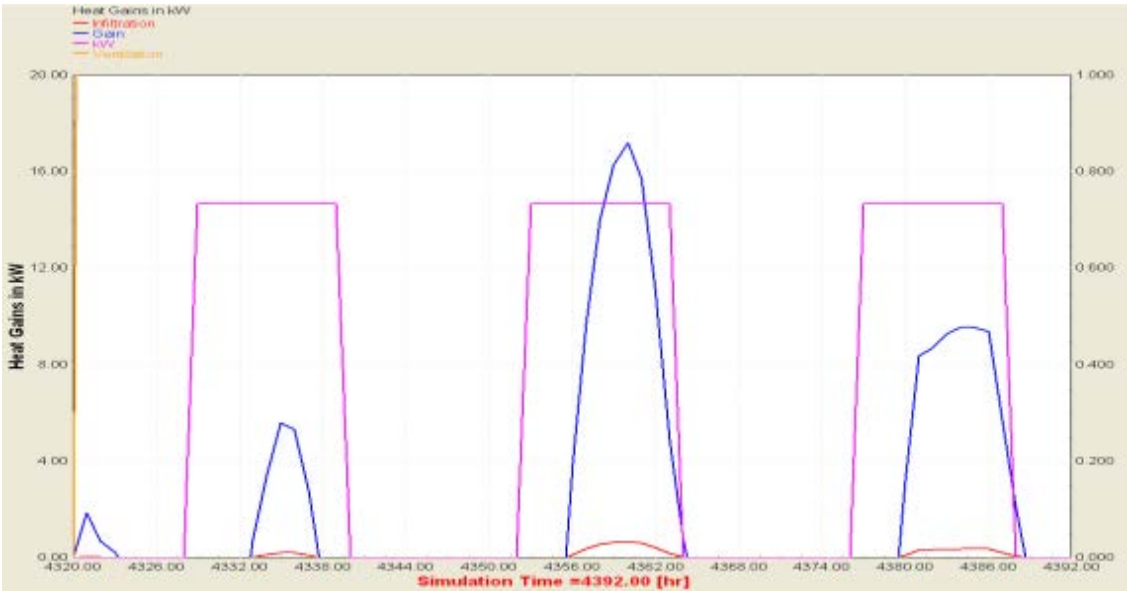

Fig 2.4.6: Heat gain curves when Ventilation is 5ACH

- Gains: If the number of persons (initial value 70) and laptops being used (initial value 70) are reduced by half to a new value of 35 each, the cooling load decreases (4-8 kW) which is same as decrease in net (sum of latent and convective) heat gain. As seen in Figure 2.4.7 and Figure 2.4.8

2.4.7: Ambient temp, office temp and cooling load curves whenGains are reduced

2.4.8: Heat gain curves when Gains are reduced

2.5 Final Cooling Load

The cooling loads were estimated with the standard configuration for selected cities. The parametric analysis conducted above was to study the impact each of these parameters on the cooling load. The cooling load of each of the selected cities was calculated at a simulation timestep of 1 hour, and simulation run time or total duration of 8760 hours i.e. 1 year. These values were stored in an output file, which would later serve as the source for cooling load during the simulation of solar based absorption system. The monthly average for daily load calculated for the selected cities is shown in Figure 2.5.1. To put the loads in perspective and for discussion, the monthly average ambient temperatures for the selected cities are also plotted in Figure 2.5.2.

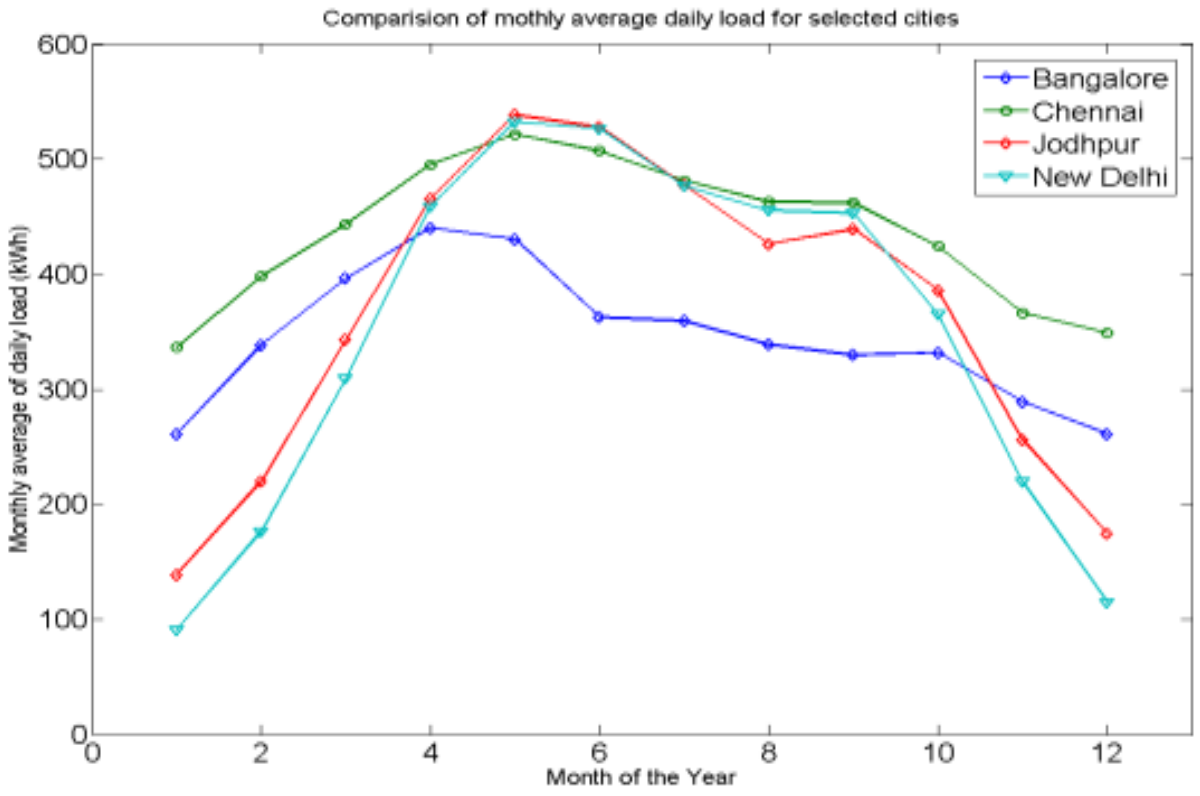

Figure 2.5.1: Monthly average of daily cooling load for selected cities

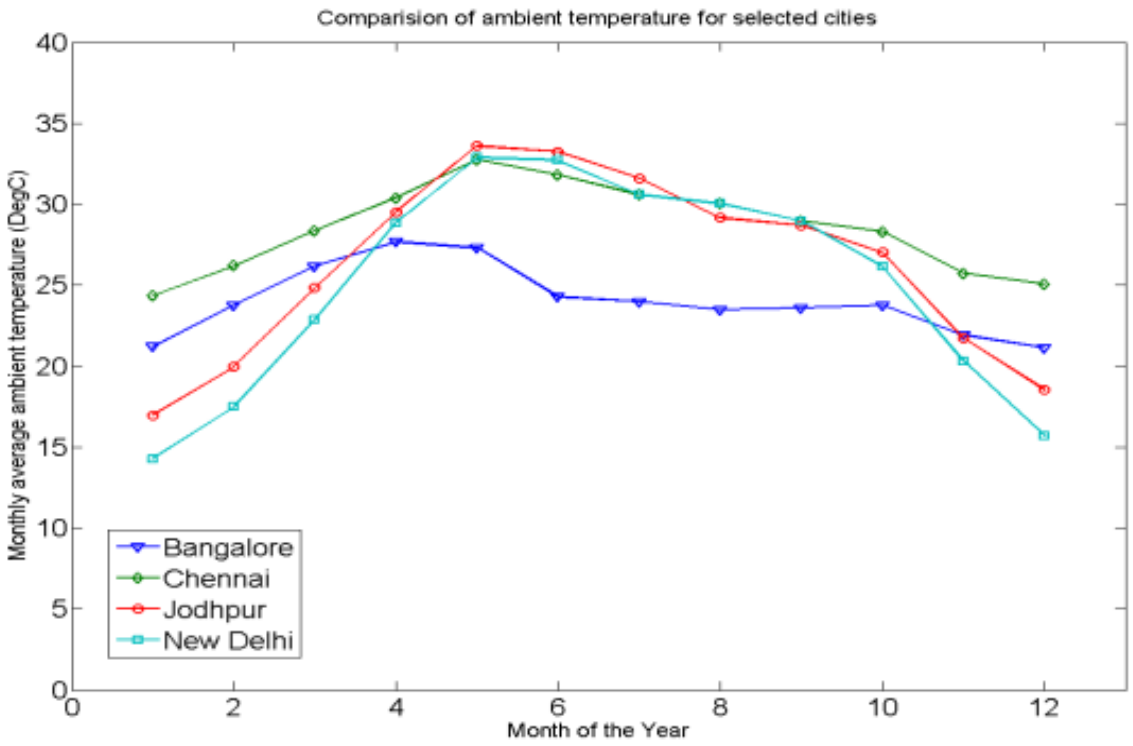

Figure 2.5.2: Monthly average ambient temperature for selected cities

The proportionality between the cooling loads and the ambient temperature is visible in the above plotted curves. The months which have highest ambient temperature for the selected cities also happen to be the ones with the highest cooling loads. This is because even if solar radiation is not the only parameter affecting the cooling load, it is the only variable for a an office premises which has other parameters more or less fixed like number of people, working hours, lighting, usage of appliances etc. The cooling loads were simulated hourly and saved in an output file. This file is used for simulating the load component in the TRNSYS model of solar absorption cycle, defined in the next chapter.

3. System Modeling

Solar based absorption cooling system was modeled using TRNSYS simulation program. TRNSYS is an acronym for a 'transient simulation program' and is a quasi-steady simulation model. This program was developed at the University of Wisconsin by the members of the Solar Energy Laboratory. It is written in ANSI standard Fortran-77. The program consists of many sub-routines that model subsystem components. The mathematical models for the sub-system components are given in terms of their ordinary differential or algebraic equations. Several standard libraries of standard components are available in TRNSYS for ease of modeling.

With the use of a program such as TRNSYS, the entire problem of system simulation reduces to a problem of identifying all the components that comprise the particular system and formulating a general mathematical description of each. The system modeled using TRNSYS can be seen in Figure 3.1. The components are modeled using different types of components in this software and with appropriate control strategies.

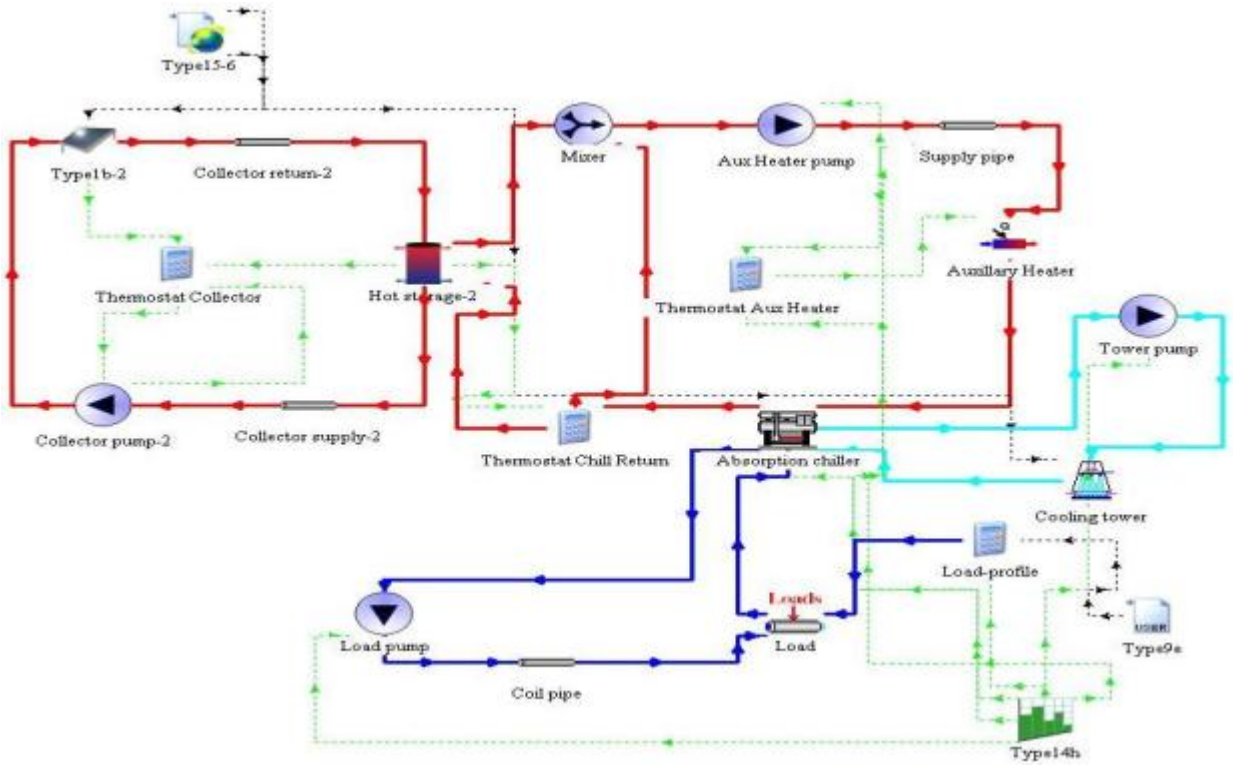

Figure 3.1: TRNSYS scheme of a solar based absorption cycle.

The simulated system, for vivid understanding can be divided into four different loops. These loops are collector loop, hot water loop, cooling water loop, and chilled water loop. Collector loop comprises of flow of hot water from storage tank to the collector via collector pump and back. Storage tank is modelled as a double inlet and double outlet tank, where one pair of inlet and outlet is used in collector loop; the other is used for hot water loop. Hot water loop comprises of the flow of hot water from storage tank to hot water inlet of chiller, through auxiliary heater and auxiliary heater pump. Cooling water loop comprises of the flow of cooling water from cooling tower to chiller and back. Chilled water loop whereas comprises of the flow of chilled water from chiller to the load and back.

The following paragraphs discusses each component, type of TRNSYS model used to simulate it, input parameters selected for it, and function in the simulated cycle. Control strategies implemented in the system are also explained as well as the reasons for selecting these specific strategies.

3.1 Solar Collector

Type1b is used to model the solar collector. It is a quadratic efficiency model which can represent any kind of solar collector, given their efficiency coefficient and incidence angle modifiers. This type also has the innate quality to represent both tracking and non-tracking type collectors. The model requires various inputs to model the collector efficiently, such as collector area, number of collectors in series, fluid specific heat, tested flow rate of the collector, intercept efficiency etc. These inputs to the collector model are obtained from the SRCC test certificates for the selected collector. By supplying data for different weather conditions using Type 15-6, to the collector model, the performance can be simulated.

The overall thermal performance of the collector array is determined by number of modules in series and the characteristics of each module. The input values to the model for collector are shown in Table 3.1.1. These are specific values for the city of Bangalore, whereas for other cities the only values different from the table are number of collectors in series and collector area. Collector area in the table represents the total collector area deployed. Apart from efficiency mode and the city specific parameters (collector area and number in series) all the parameters are taken from the SRCC test results of the selected collector. The efficiency mode value is selected as 1,

which represents the fact that the efficiency parameters are given as a function of the inlet temperature to the collector.

Name	Value	Unit
Number in Series	8	-
Collector Area	908	m^2
Fluid Specific Heat	4.19	kJ/kg.K
Efficiency Mode	1	-
Tested Flow rate	72	$kg/hr.m^2$
Intercept efficiency	0.671	-
Efficiency slope	0.4674	$W/m^2.K$
Efficiency curvature	0.03234	$W/m^2.K^2$
1st order IAM	0.287	-
1nd order IAM	0.344	-

Table 3.1.1: Input parameters for Collector Model

	Chiller Model: YAZAKI WFC-SC20		
	Cooling Capacity	70.3	kW
	Rated C.O.P	0.699	-
Chilled water	Inlet temperature	12.5	C
	Outlet temperature	7	C
	Rated flow rate	11	m^3/hr
Cooling water	Inlet temperature	31	C
	Outlet temperature	35	C
	Rated water flow	36.7	m^3/hr
Heat water	Inlet temperature	88	C
	Outlet temperature	83	C
	Inlet temperature range	70-95	C
	Rated water flow	17.3	m^3/hr

Table 3.3.1: Parameters for YAZAKI 20 Ton Chiller

3.2 Storage Tank

Type4a is used to model the storage tank. This type can be used to model storage tanks with fixed inlets and uniform losses. The loss coefficient value for the storage tank is a crucial parameter while simulating it, as it impacts the retention capability of the storage tank. The loss coefficient for this study was assumed to be 20 $kJ/hr.m^2.K$, as this is a more realistic value (Suter, J.-M). This value for the loss coefficient can be further reduced by careful design. Type4a can also be used to represent a stratified storage tank, for this thesis the tank model was stratified into 10 layers of 0.3m height each.

The volume of the tank is another crucial parameter. This is because it determines the number of hours of buffer energy provided by the tank. The sun hours at the selected cities is not expected to be more than 6 to 7 hours, whereas the cooling load is simulated for 11 hours a day i.e., the working hours of an office premise. This creates a demand for a longer duration, but on the other hand energy collected from collectors at peak radiation hours is more than required to supply the cooling load. In addition, during partly cloudy days, availability of solar radiation can be

intermittent. This makes the incorporation of storage tank important in a solar based absorption system. The initial value for tank volume is set so as to provide a buffer of 2 hours, which was concluded to be the optimum value by Ming Qu(Qu, Ming, 2009) . This value was calculated to be 14m^3.

3.3 Chiller

Type107 is used to model the absorption chiller for this study. This type represents a hot water fired single effect absorption chiller. Since the capacity was decided to be 20 Tons, and the model selected for this study was SC20 from the maker YAZAKI, the datasheet for this type was used to define the input parameters for the simulation component. These parameters are specified in Table3.3.1. Data sheet of SC20 from which these parameters are taken can be easily downloaded from the company website.

This TRNSYS model uses a normalized catalog data lookup approach to model a single-effect hot-water fired absorption chiller. "Hot Water-Fired" indicates that the energy supplied to the machine's generator comes from a hot water stream. The model computes the capacity and design energy input fraction based on four input parameters. These parameters being fraction of design load, chilled water setpoint, cooling water inlet temperature, and inlet hot water temperature to the chiller. All these computations are done for a hot water inlet temperature range of 90 to 115 DegC and stored in a data file. This data file is referred to by the model during simulations. The data file values are either experimental values or interpolated for different values of the parameters. Since this data file is normalized, it can be used for other ranges as well range. Hence the data file was modified to the specific hot water inlet conditions of the selected model i.e. 70 to 95 DegC.

3.4 Pumps

The pumps in the system are modeled using Type114, a single speed pump. As seen in the simulation scheme, there are four pumps used in this simulation of solar based absorption cycle. The flow rates of these four pumps are different and calculated based on the requirements of the components they're serving. The flow rate through the pump in the collector loop is defined by the total flow through the collector array i.e., the product of rated flow for a single collector and the number of collector rows in parallel. Whereas the flow rate through the pumps in auxiliary heater circuit, cold water circuit and cooling water circuit is defined by the flow rates required of

respective flows in the chiller model. The flow rates through the pumps can be seen in Table 3.4.1. There are no energy or flow rate losses assumed in the pumps, which would not have much effect on the analysis as stated in the next chapter. The outlet temperatures of the pumps are an active part of the control strategies being implemented in different loops of the system.

	Flow rate	Unit
Collector Pump	15000	kg/hr
Aux. heater pump	17280	kg/hr
CW pump	36720	kg/hr
Chilled water pump	10980	kg/hr

Table 3.4.1: Flow rates through pumps in system

3.5 Cooling Tower

The cooling tower required for the solar based absorption cycle is modeled using Type51a, which works on an external data file. The component is modeled as a counter-flow device, with a single tower device. The cooling water flows from the outlet of cooling tower to the chiller model, where it absorbs the discarded energy by the chiller and then returns to the cooling water. Since inlet temperature of the cooling water is a parameter affecting the efficiency of the chiller, the cooling tower serves as a critical component to the cycle. This temperature can either be maintained by varying the air flowrate through the tower based on inlet cooling water temperature or by maintaining a high air flowrate. By maintaining a high air flow rate such that it is sufficient to maintain the desired outlet temperature of the cooling water, the cooling tower can be excluded from the study as a variable parameter affecting the system analysis.

3.6 Load

The cooling load simulated using TRNBuild for each city is written in a file and read using Type9e reader in this SBAC simulation. The values read from Type9e are converted into appropriate units and then given as input load into the cold water circuit. Figure 3.6.1 shows hourly cooling load profile for Bangalore, over 8760 hoursi.e one year. Similarly the cooling loads for other cities were read from their respective output files. The absence of cooling load at night time i.e. after working hours should be visible as gaps, but this cannot be seen in Figure 3.6.1 as the simulation time for this curve is 8760 hours. These gaps can be observed in Figure 2.4.1 where cooling load is plotted over a smaller simulation time of 72 hours.

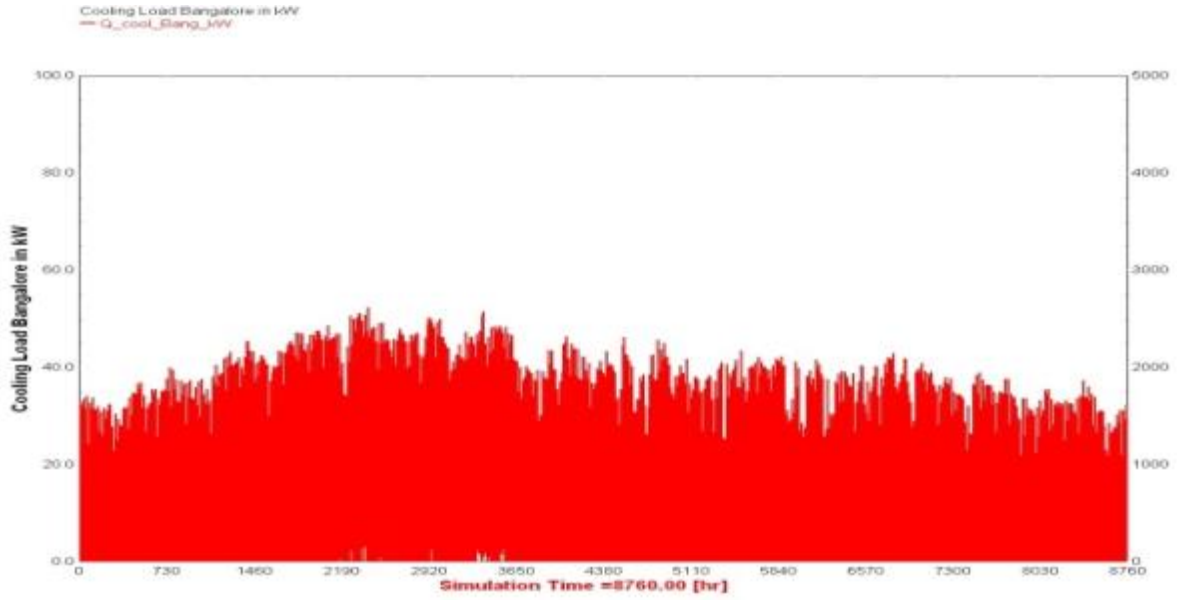

Figure 3.6.1: Hourly cooling load profile for Bangalore

3.7 **Forcing Function**

A time dependent forcing function is imposed on the system to follow the "workday" timings of 08:00 to 19:00 hours, which are followed while calculating the cooling load in TRNBuild. Hence Type14h implements a forcing function which shuts off the components after working hours, irrespective of their individual control signals. Hence, this serves as the master control for the components to switch off as there is no requirement at the load end of the cycle.

3.8 Control Strategies

Thermostats are used to implement the control strategies of the system. There are three control strategies being used in the system, to control the flow through the collector, to control the hot water outlet from the chiller, and to control the functioning of the auxiliary heater being used. Each of these control strategies employs a different thermostat. The functioning of these thermostats are as follows:

- Collector Thermostat: The function of the collector thermostat is to manage the flow through the collector. Since the collector pump is a single speed pump, the flow can either be the rated flow or zero. This thermostat provides the control signal to the

collector pump, after determining whether the pump should be switched OFF or ON for the particular time step of the simulation.

The flow through the collector needs to be regulated for two reasons. One is to maintain the outlet temperature of the collector, which should not attain boiling temperature. As the system is working on atmospheric conditions, the outlet temperature of the collector should be kept below 100 DegC in all cases. This could be overcome with including a relief valve in the system, but in this study the control strategy is to focused on maintain the temperature by controlling the flow through the system. So a check was implemented on the outlet temperature of the collector using the thermostat.

Second reason why the flow needs to be regulated is so that the fluid doesn't lose energy to the surrounding through the collector, instead of gaining it. This would happen when inlet fluid to collector is at a higher temperature than the outlet fluid. This situation can be avoided by putting in a condition for the flow to only take place when the outlet temperature of the collector is higher than the inlet temperature.

Solutions to both the problems stated above should both be implemented, which makes a singular condition at which the water flow through collector should be allowed by controlling the collector loop pump. Hence, the condition at which the collector pump works is :

- Temperature of inlet water to the collector is lower than temperature of outlet water of collector (T_collector_out>T_collector_in)

  AND
- Temperature of the outlet water of collector is less than 98 DegC (T_collector_out< 98)

It was observed that if the temperature of fluid in storage tank's top layer replacesoutlet temperature of fluid from collector in the second part of the condition stated above, during this control strategy, the solar fraction of cycle increases. The explanation for which can be that since for this study single speed pumps were chosen, during the time

when collector pump was in OFF state, there was no flow through collector. This made the outlet temperature of collector rise steeply, as collector flow was zero off but solar radiation was at its peak value.

This rising temperature was often more than maximum outlet temperature allowed as per the above condition, which would shut off the pump and a lower solar energy would be collected. Lower solar energy meant higher energy required from auxiliary heater, which can be noticed by referring to Figure 3.8.1 and Figure 3.8.2. In these plots, solar energy (pink) and auxiliary energy (light green) required are plotted over a simulation time of 72 hours. Figure 3.8.2 shows a peak of 25kW of auxiliary energy at 42hours timestep and couple more peaks at close approximations of 66hours timestep value. No such peaks of auxiliary energy required are seen in Figure 3.8.1, which represents the case when temperature of outlet water from collector is replaced by temperature of hot water at top layer of storage tank.

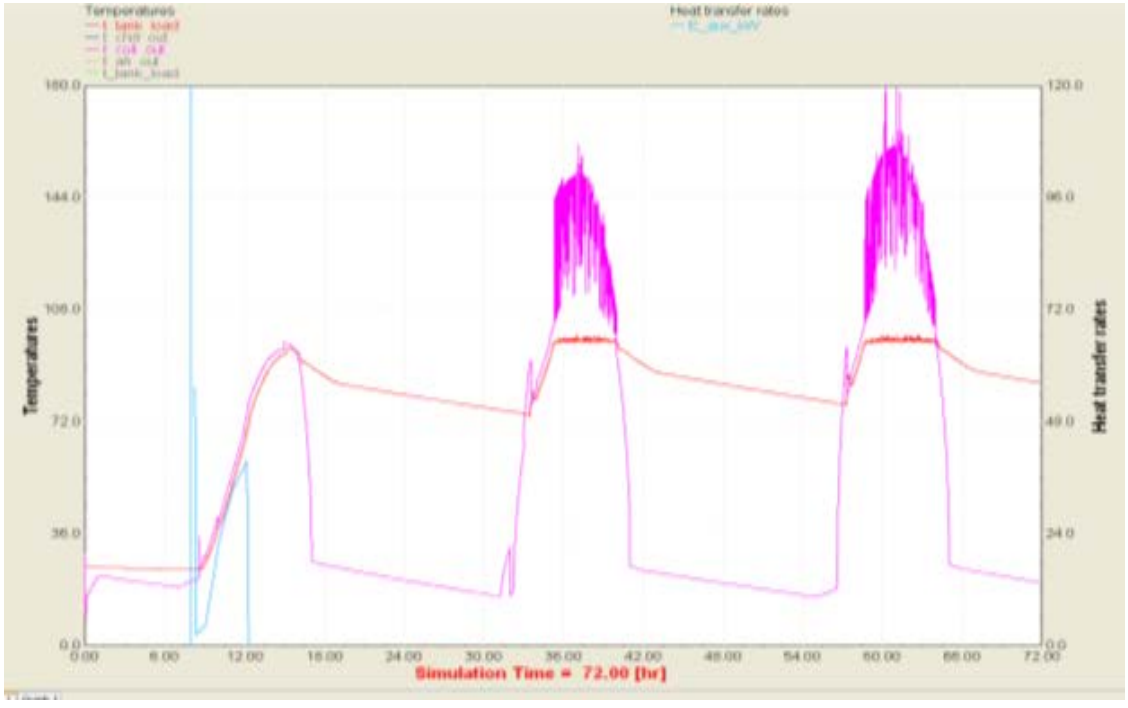

Figure 3.8.1: Solar and auxiliary energy curves with T_collector_out in the control strategy

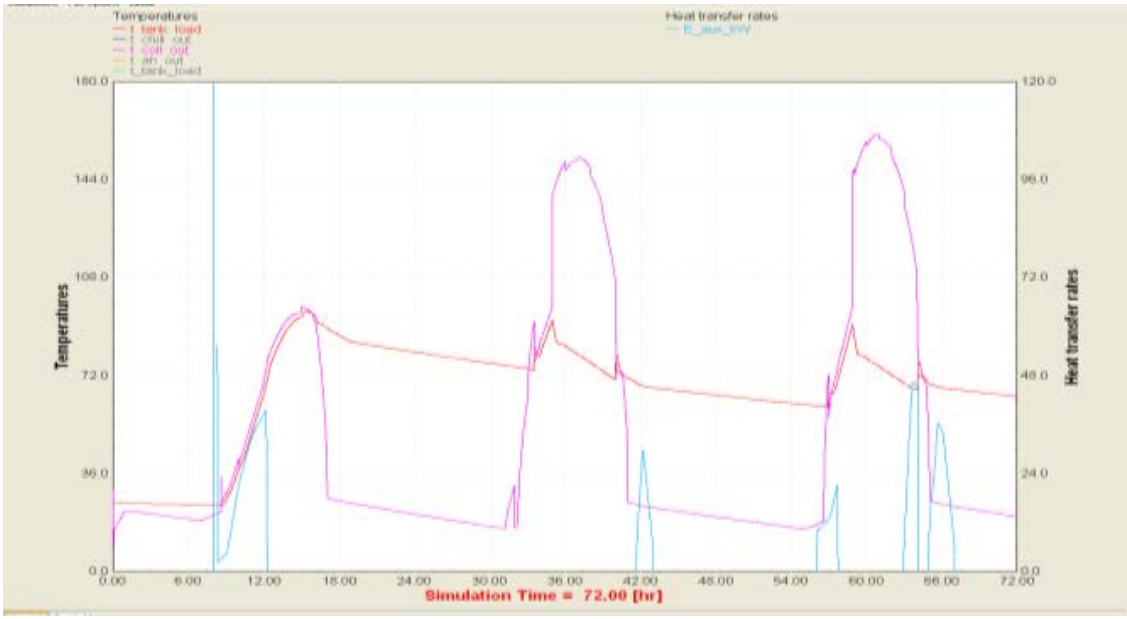

Figure 3.8.2: Solar and auxiliary energy curves with T_toplayer_tank in the control strategy

- Auxiliary Heater Thermostat: This thermostat is used to regulate the control signal required for functioning of the auxiliary heater. It controls the maximum temperature at which the auxiliary heater starts functioning, and the temperature to which the heater heats the fluid. The temperature at which auxiliary heater starts functioning is referred to as “kick-in” temperature and the temperature to which the heater heats the fluid is referred as “set point” temperature.

  If the inlet temperature is higher than the “kick-in” temperature then the heater is switched off and the fluid simply passes through the heater without any temperature drop. Both the temperatures are given as the same values in our study.

These set point temperatures play a vital role in the performance of the system. Figure 3.8.3 represents the variation in monthly solar fraction for different values of temperature settings, specifically for Bangalore. The lower the temperature setting of the auxiliary heater, the sooner it starts contributing energy to the cycle and the lower the fraction of energy from collectors become. For this study a set point temperature of 80 °C was selected for the auxiliary heater thermostat. This temperature is neither the lowest working temperature for the selected chiller model, nor the highest. Although it should be noted that this set point temperature indicated the minimum temperature at

which the hot water will be delivered to the chiller, not the highest. The highest temperature for the hot water inlet is controlled by the fact that collectors are not working beyond a certain outlet temperature, which for this study is 98 °C.

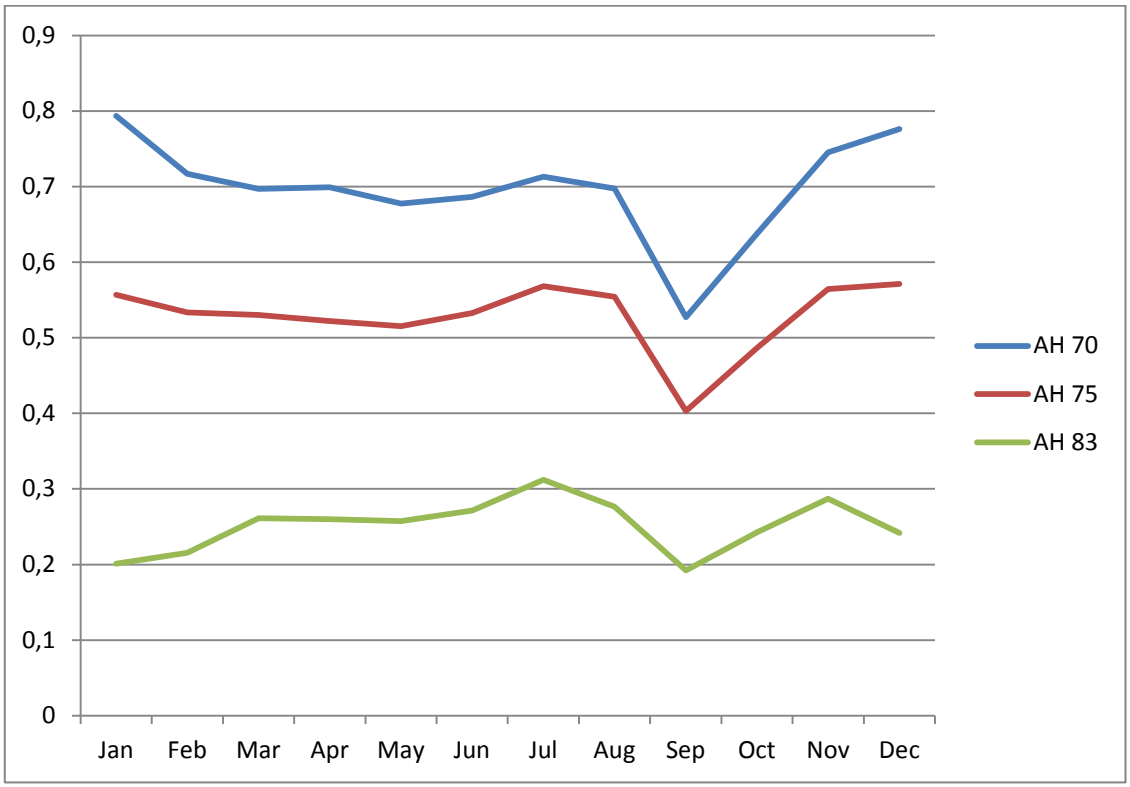

Figure 3.8.3: Variation in monthly solar fraction with changing Auxillary Heater temp (AH) for Bangalore

- Chiller Return Thermostat: This control strategy was implemented in the hot water loop to improve the solar fraction for the simulated cycle. The control strategy comprised of not supplying hot water from storage tank to the chiller till it is completely charged i.e. possesses contains hot water at 80 °C temperature, which has previously been defined as the setting temperature for auxiliary heater thermostat. This thermostat can be seen in Figure 3.8.4, which depicts only the hot water loop of the simulated cycle.

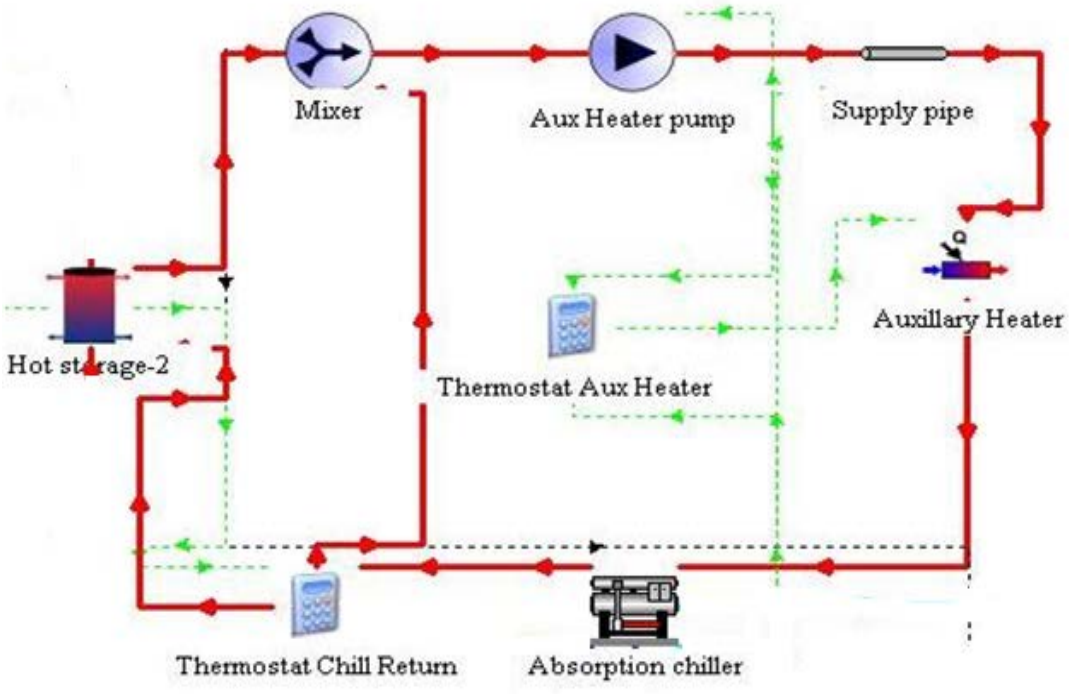

Figure 3.8.4: Hot water loop of simulated cycle with chiller return thermostat

Instead, flow from outlet of hot water from chiller is diverted back to hot water inlet side of the chiller. The flow from outlet of hot water from the chiller if is at a higher temperature than the hot water in the storage tank, then mixing this water with the tank water will indeed be a loss of energy. Hence there is a thermostat which makes the flow of water in hot water loop bypass storage tank if it is at a higher temperature than its counterpart in storage tank. This thermostat is referred to as the chiller return thermostat in the remaining thesis. The effect of this control strategy can be stated through quoting the finding that increase in annual solar fraction with strategy was over 50%. This can be noticed by glancing through Figure 3.8.5 and Figure 3.8.6, which have annual solar fraction plotted “without” and “with” this control strategy in the cycle. The red curve in the plots represents the annual solar fraction, which is plotted on Y axis.

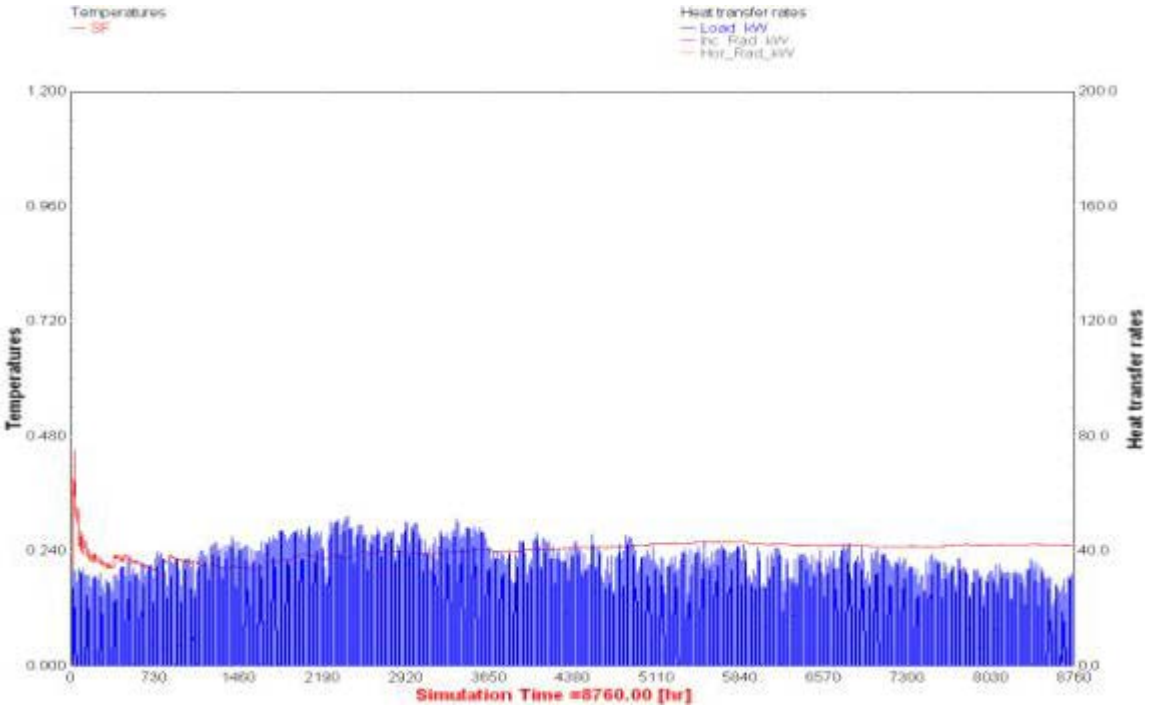

Figure 3.8.5: Annual solar fraction over cycle simulation without chiller return thermostat

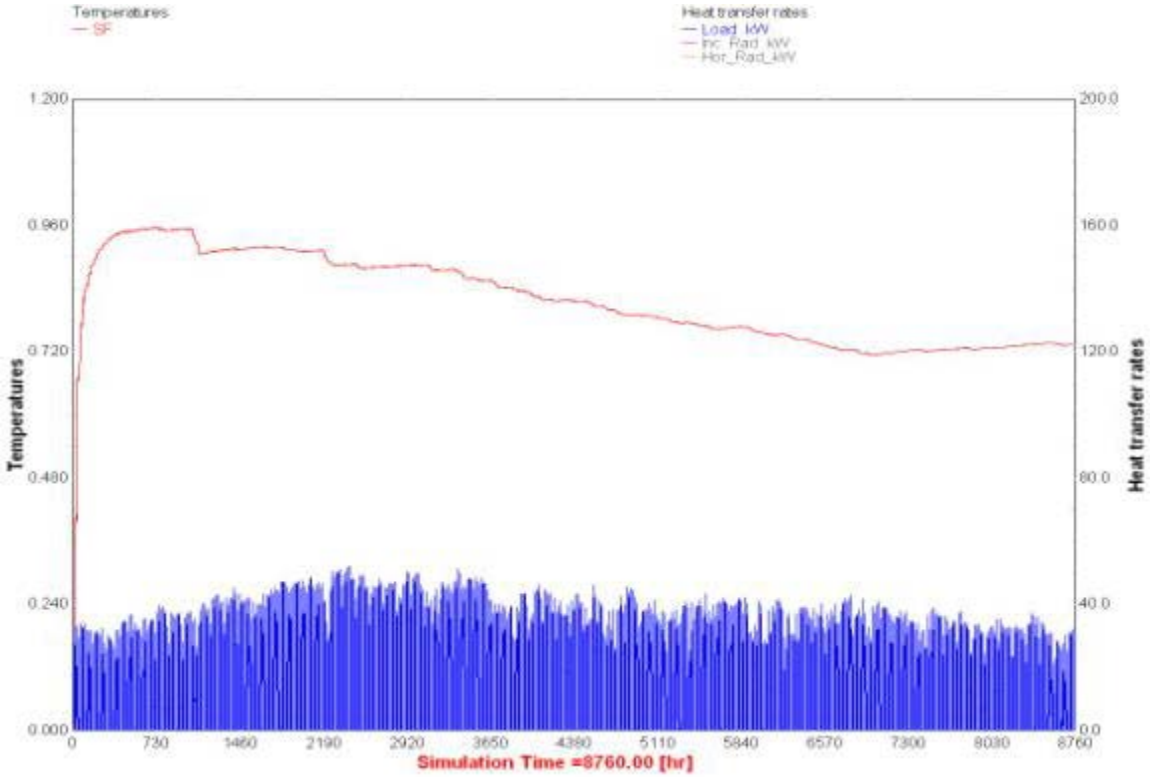

Figure 3.8.6: Annual solar fraction over cycle simulation with chiller return thermostat

Solar based absorption cycle was simulated with detailed specifics of the components of the cycle and control strategies. The aim was to optimize key parameters affecting the performance of the system. This was done using parametric analysis and Life Cycle Savings (LCS) analysis in the next chapter.

4. System Analysis

There are multiple parameters which affect performance of the simulated solar absorption cycle. These parameters can be sizes of certain components (collector area or storage tank volume), or some specific characteristic (flowrate or collector slope). During simulation of the system, these parameters were given values which are standard and reasoning was provided as to why these values were selected. These initial values of the parameters used in the TRNSYS model are either based on actual facilities or obtained from the research found in literature. The values given to these parameters can be referred to in Table 4.1. Next step in this study was to optimize these parameters to achieve more efficient cycle and reduce losses. Hence, parametric optimization process with the aim of finding ideal sizes of the components and related parameters is conducted by performing various iterations on the TRNSYS model described in Section 3.0. Multiple runs of simulation are performed on the TRNSYS model using MATLAB code. This MATLAB code written to perform iterations for varying parameters is the basic code used during this study. Several modifications were made to this code for each parametric analysis conducted, simplest one being to modify the parameter under analysis with the loop variable. In case two parameters were iterated for the same analysis, nested loops were included in the code. This MATLAB code, and an explanation for it can be found in Annexure I.

Important Variables and Standard Values		
Variable	**Value**	**Unit**
Collector Area (Bangalore)	980	m^2
Collector Slope	12.98	°C
Collector Flowrate	15000	kg/hr
Storage Tank Volume	14	m^3
Hot Water Flowrate	17280	kg/hr
Aux Heater Kick-In Temp	<80	°C
Aux Heater Setting Temp	80	°C
Chiller Hot Water Inlet	>= 80	°C
Chilled Water Flowrate	10980	kg/hr
CW Flowrate	36720	kg/hr
Chilled Water Set Point	7	°C

Table 4.1: Values of parameters in initial simulation for Bangalore

Before explaining the results obtained from parametric analysis, the reader should be made familiar with certain terms used during the analysis. These are as follows:

- Heater energy required: This is the energy supplied by the auxiliary heater to run the absorption chiller. Auxiliary heater only supplies energy when storage tank is not sufficiently charged i.e., cannot supply hot water at a minimum temperature of 80 °C. Since water in the storage tank is heated by gaining energy from the collectors, it can be stated that solar energy is the only component charging the storage tank. The sum of the energies supplied by collectors and auxiliary heater is the total energy input required to run the absorption chiller during the cycle.
- Useful solar energy required: The term solar energy represents the energy collected by the collectors and then supplied to hot water in storage tank. Since this term does not account for the energy losses at storage tank or at other steps of the cycle, it gives an inflated value for the solar energy actually used to run the absorption chiller. This in turn gives results which have not taken the losses into account. Hence, for this study solar energy is calculated as the difference between total energy required by the absorption chiller and energy supplied by the auxiliary heater. Since this term only considers the "useful" part of solar energy in the cycle, it was termed as useful solar energy required.
- Solar fraction: It is taken to be the part of the generator load that can be covered by the solar energy. Generator load is the sum of useful solar energy and auxiliary heater energy, hence solar fraction can be stated as:

$$Solar\ Fraction\ (sf) = \frac{useful\ solar\ energy}{generator\ load}$$

$$= \frac{useful\ solar\ energy}{useful\ solar\ energy + auxilary\ heater\ energy}$$

Solar fraction by definition represents the fraction of generator load supplied by the solar energy and it is this parameter which has be maximized to optimize the cycle. Whereas on the other hand, auxiliary heater energy being inversely related to the useful solar energy is the parameter which should be minimized. The variation of these three terms is the analyzed while performing parametric analysis on the key parameters. During technical analysis it is found that collector area, a key parameter affecting these terms cannot be optimized by parametric analysis alone. It is also

found that optimum storage tank volume is dependent on the collector area. Hence to optimize these two key parameters of the given system, Life Cycle Savings (LCS) analysis is also performed.

4.1 Parametric Analysis

It should be reminded to the readers that the parametric analysis is performed not only to optimize the key parameters, but to optimize these for each of the selected cities. As stated before, the selected cities have different incident solar radiation and weather conditions. Figure 4.1.1 shows the monthly average of daily radiation incident on these selected cities. It can be seen that Jodhpur and New Delhi, both being cities with higher latitude and non-coastal climate have similar irradiation trends. Whereas Bangalore and Chennai, both having lower latitude and tropical climate have lower solar irradiation when compared to the former. All the four cities observe a drop in irradiation during 7^{th} and 8^{th}months i.e. (July and August); this can be attributed to the monsoons in India. Monsoons range from June to November, depending on the city´s location in the subcontinent. It is also observed that the peak irradiation for all the four cities if for the months of April and May.

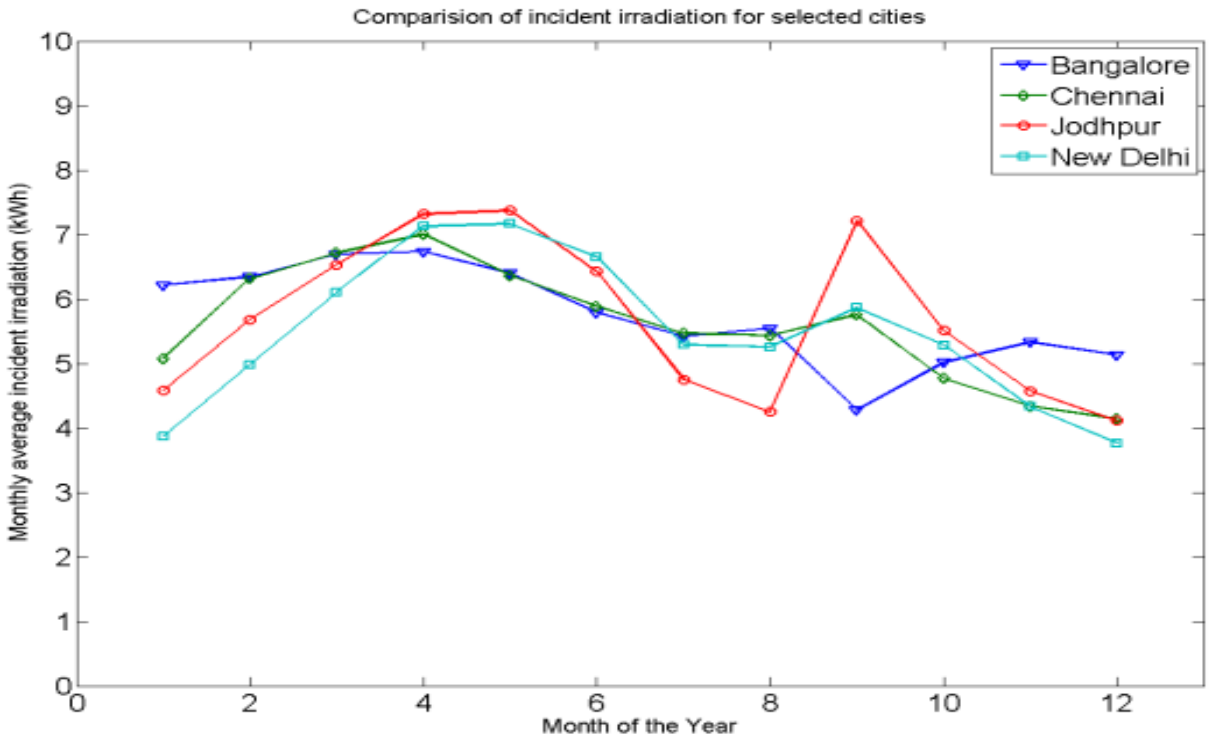

Figure 4.1.1: Monthly average of daily incident solar irradiation on collector plane for the selected cities

In the Figure 4.1.1, a sharp decrease is noticed in the incident irradiation for the month of September at Bangalore. Relating to the trend of monthly solar fraction in Figure 2.5.1, a decrease is also noticed for the month of September at Bangalore. But this decrease is not noticed in Figure 2.5.2, which means that solar fraction being a direct depiction of incident irradiation would show similar trends whereas the cooling load depends on a number of factors and incident irradiation is just one of them. Hence the similar decrease for the month of September is not noticed while observing the trend for cooling load at Bangalore.

Although the optimization can be based on many parameters, three key parameters were selected for this study. The parameters selected, and the reasoning behind their selection is as follows:

- Collector area: Total area of the collectors installed is a crucial parameter, as the useful solar energy is directly proportional to this parameter.
- Collector slope: The angle of inclination of the collectors plays a significant role on the solar irradiation incident normal to the surface of the collector.
- Storage tank volume: The storage tank is included in the system as a buffer, but the optimum value of this tank is very crucial as explained later.

Parametric analysis was performed on these three parameters to maximize solar fraction and useful solar energy required. Maximization of useful solar energy would minimize auxiliary boiler energy required, as they are inversely related. The result of the analysis for each of the parameter is discussed below.

4.1.1 Collector Area.

Collector area was varied from 0 to 1000 $m^2$for this analysis. Although the values for $CA_{max}$are different for selected cities, same range of values was used to perform comparative analysis for selected cities. The variation of annual solar fraction with varying collector area can be seen in Figure 4.1.2. It is observed that the solar fraction increases with increase in collector area, but the effect of increasing collector area is more significant only till 500 m^2. After 500 m^2 collector area, the slope of increase of annual solar fraction decreases with increasing collector area. Similar trend is noted for useful solar power, as observed in Figure 4.1.3.

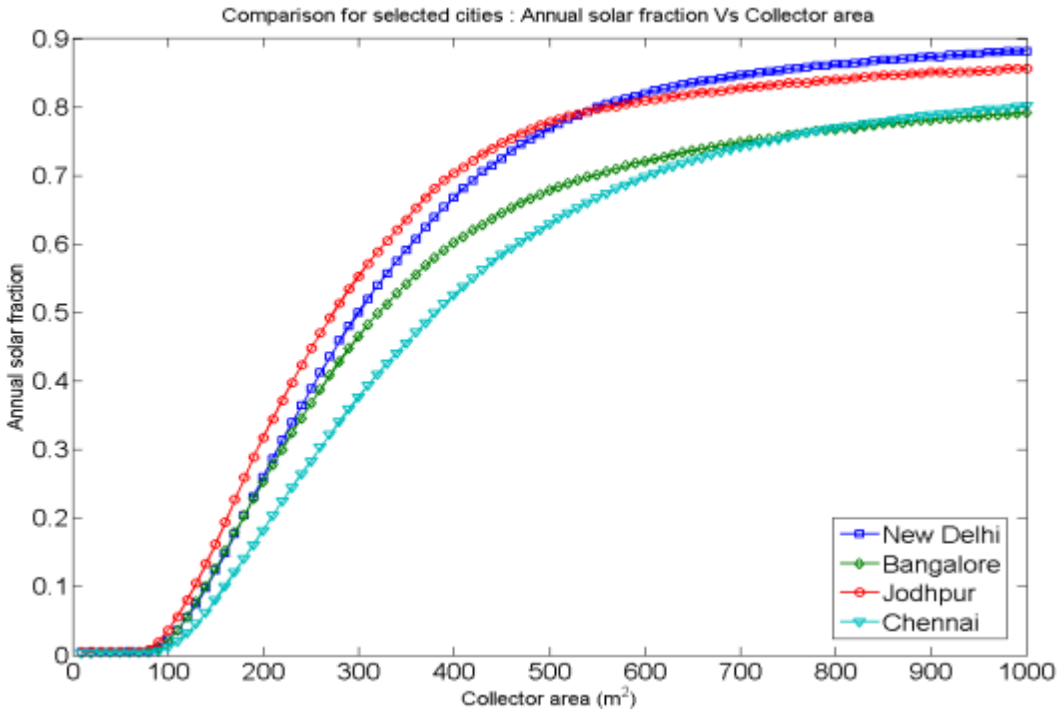

Figure 4.1.2: Annual solar fraction Vs Collector area

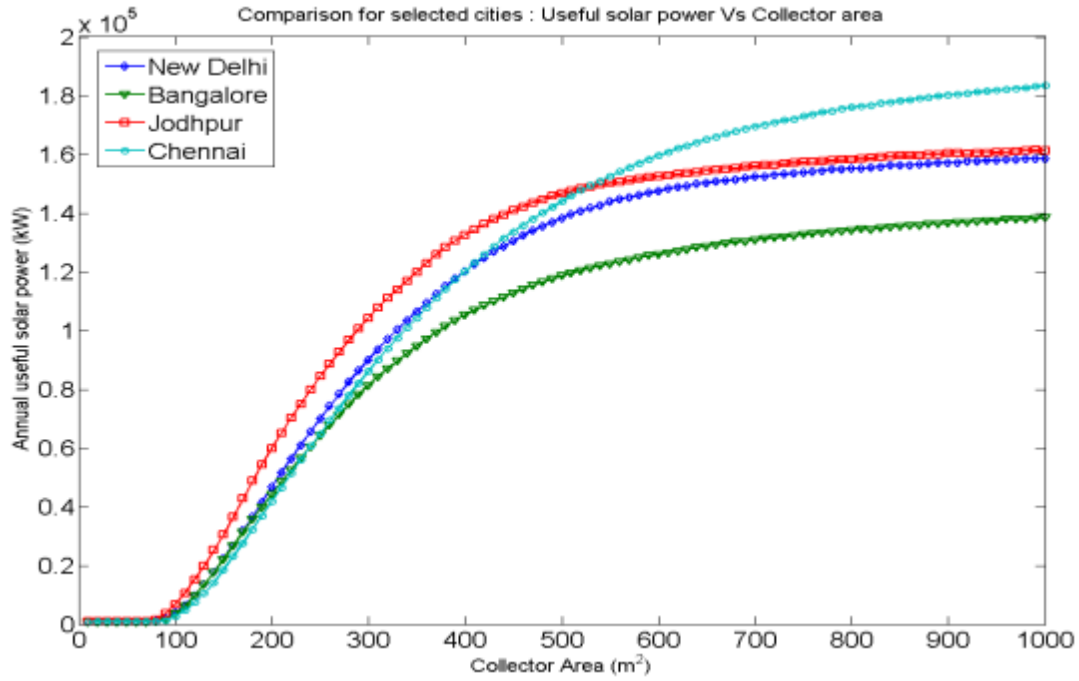

Figure 4.1.3: Annual useful solar power Vs Collector area

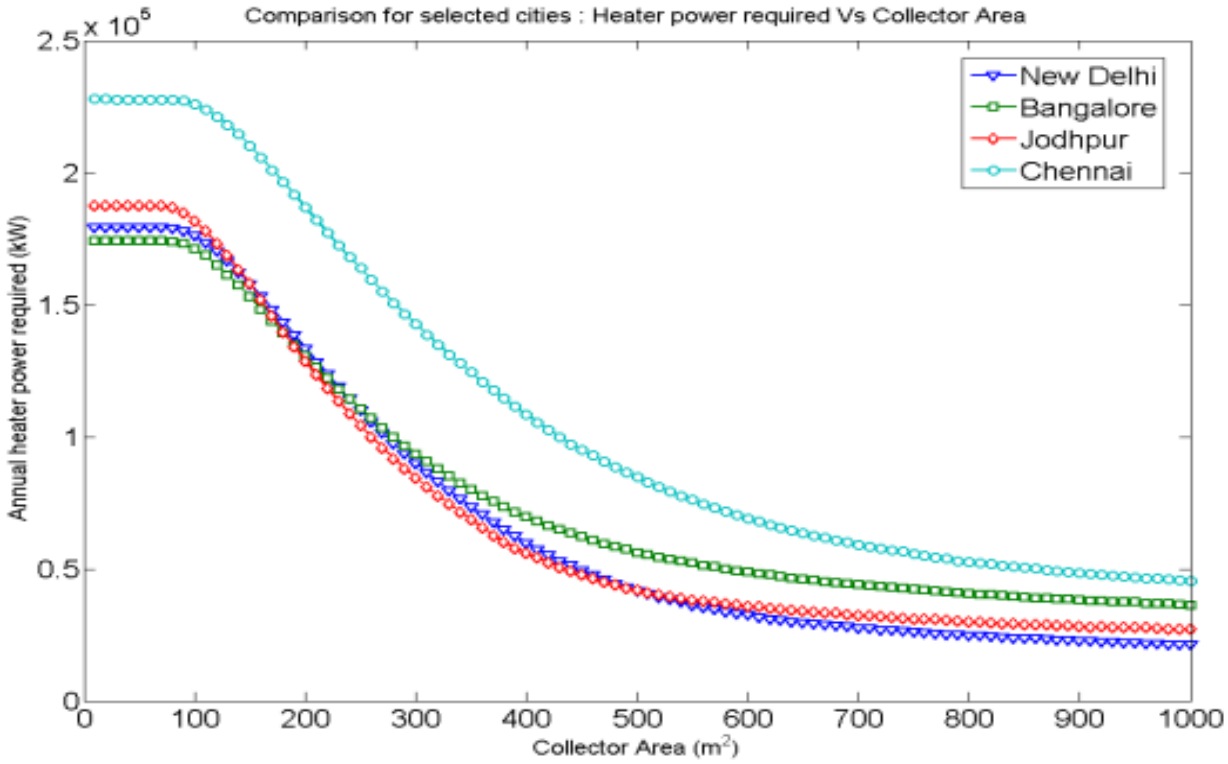

Figure 4.1.4: Annual heater power required Vs Collector area

As expected heater power required shows an opposite trend to that of the useful power and solar fraction. Heater power required decreases with increase in collector area, whereas the slope of decrease is not the same through the range of collector areas. The slope of decrease of heater power required is higher till 500 m^2 and then the rate at this heater power was decreasing, decreases. This can be observed in Figure 4.1.4.

It can also be noted in the above plots that till the range of 100 m^2 of collector area, useful solar power gained is insignificant completely. Due to which solar fraction is also zero till collector area of 100 m^2. The reason for this can be attributed to the auxiliary heater kick in temperature or the auxiliary heater thermostat setting temperature (AHT). The values for which is 80°C for these simulations. This means that collector area is not sufficient enough to heat up the water in the storage tank of assumed size to this temperature, so auxiliary heater provides all the energy required to supply the generator load. This can be understood from the solar fraction plots with varying collector area with Auxiliary Heater Temperature (AHT) as 70 °C and AHT as 85 °C. The Figures representing the respective plots are Figure 4.1.5 and Figure 4.1.6.

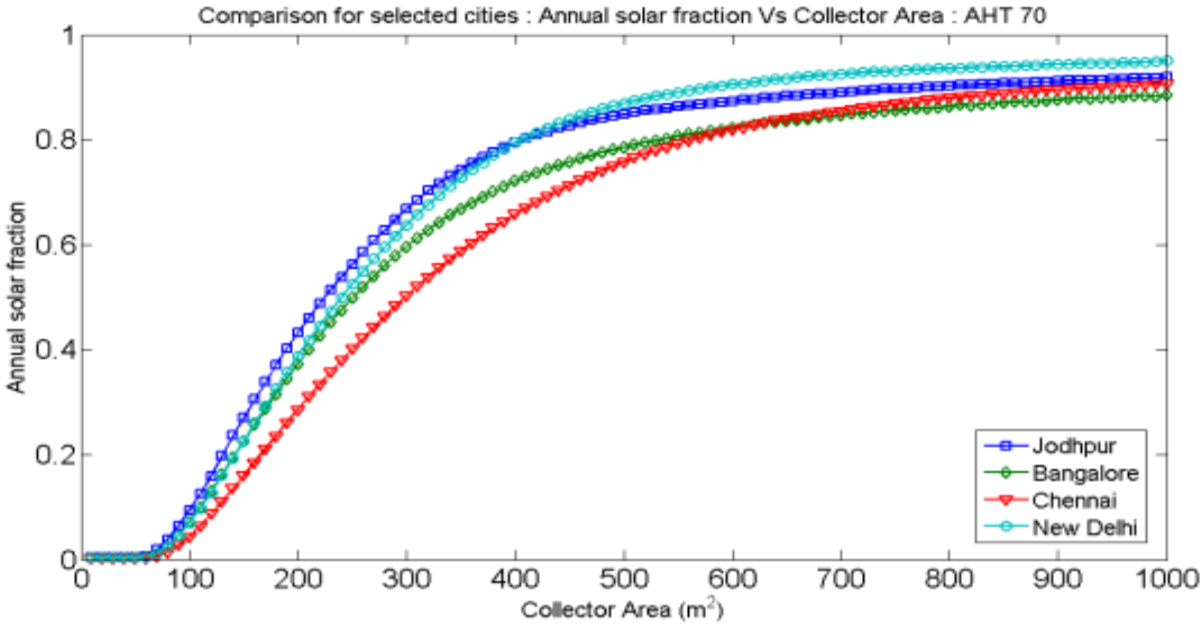

Figure 4.1.5: Annual solar fraction Vs Collector area with AHT as 70°C

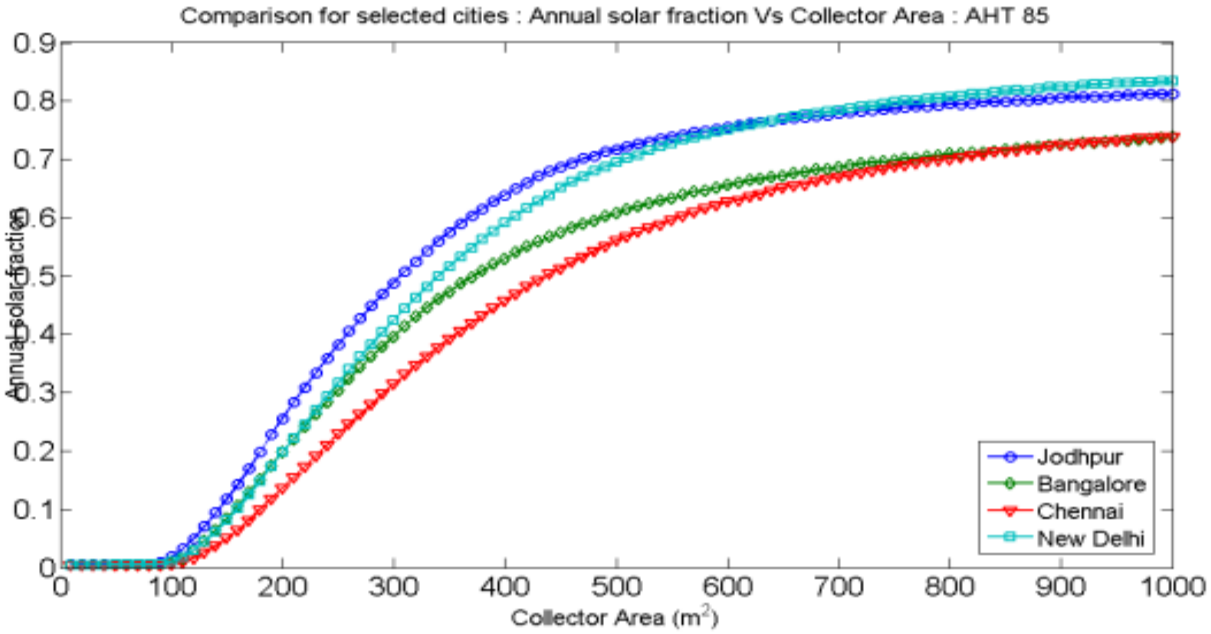

Figure 4.1.6: Annual solar fraction Vs Collector area with AHT as 85°C

In these plots it can be seen that the annual solar fraction at 100 m^2 is more when AHT is set to 70 °C, in comparison to the case when it is set to 85 °C. This difference can be seen more prominently in Figure 4.1.7 and Figure 4.1.8, showing a zoomed in view of these plots till a collector area range of 200 m^2.

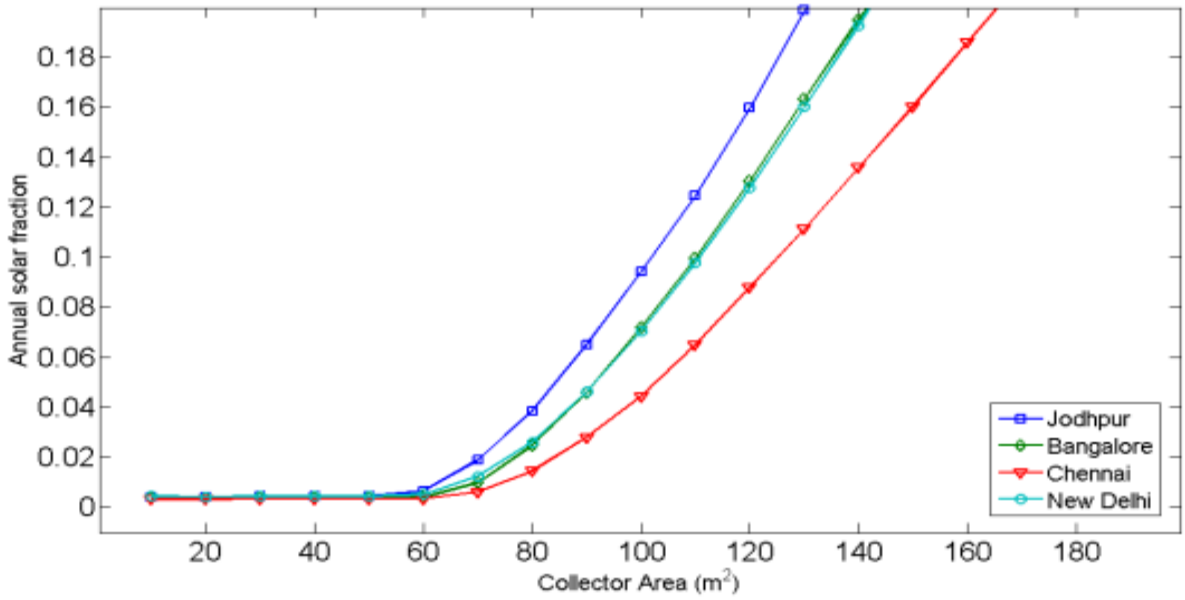

Figure 4.1.7: Zoomed in view ofannual solar fraction Vs Collector area with AHT as 70DegC

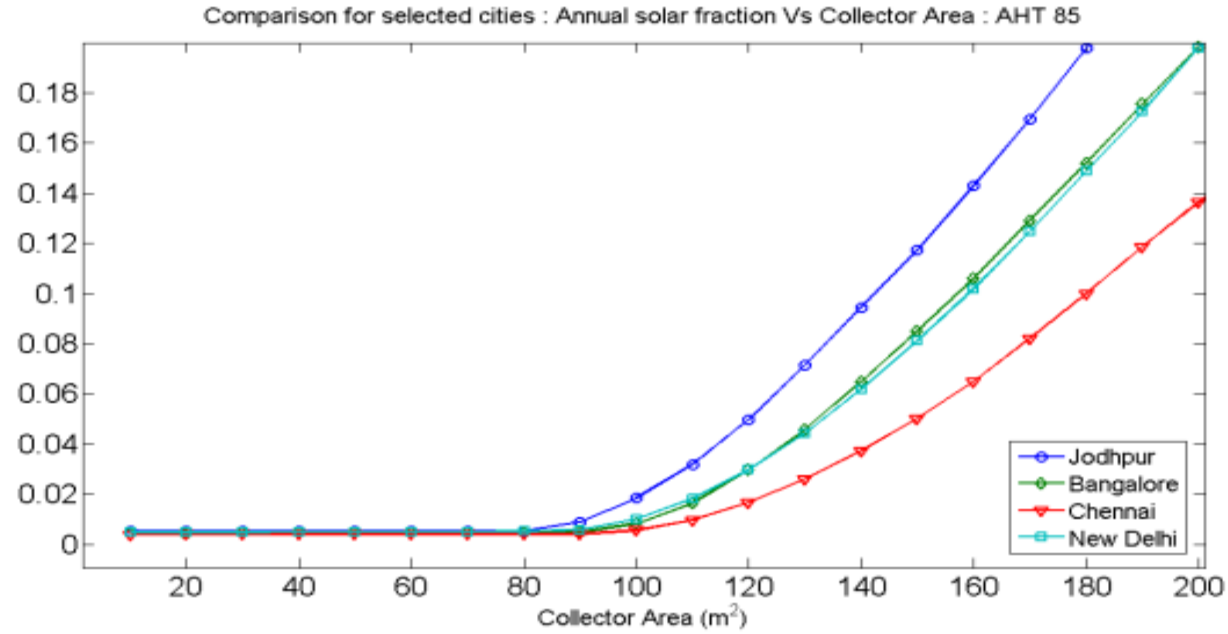

Figure 4.1.8: Zoomed in view ofannual solar fraction Vs Collector area with AHT as 85DegC

With the parametric analysis based on collector area, no optimum value of the collector could be achieved. Although it can be said that the value would be close to 500 mark, as this is where the gradient of increase in solar fraction or useful solar power decreases. Hence, LCS analysis was conducted, as mentioned in detail later on in this chapter.

4.1.2 Collector Slope

The selected collector is a non-tracking collector and by theory the optimum value to collector slope for a non-tracking collector should be the latitude of the location of the collector. Taking into account other factors, such as more irradiation during early months of the year for Bangalore or climatic conditions of the particular city, it was decided to conduct parametric analysis for collector slope too. Collector slope was varied for the analysis within the range of 0° to 30°. Figure 4.1.9 shows the variation in auxiliary heater power required while changing the collector slope for the city of New Delhi. It can be seen that that there is not much difference between the auxiliary heater power required for collector slope values of between 25° to 30°. However the minimum value of auxiliary heater power is for collector slope of 28.1°, which is close to the latitude of New Delhi i.e. 28.6°.

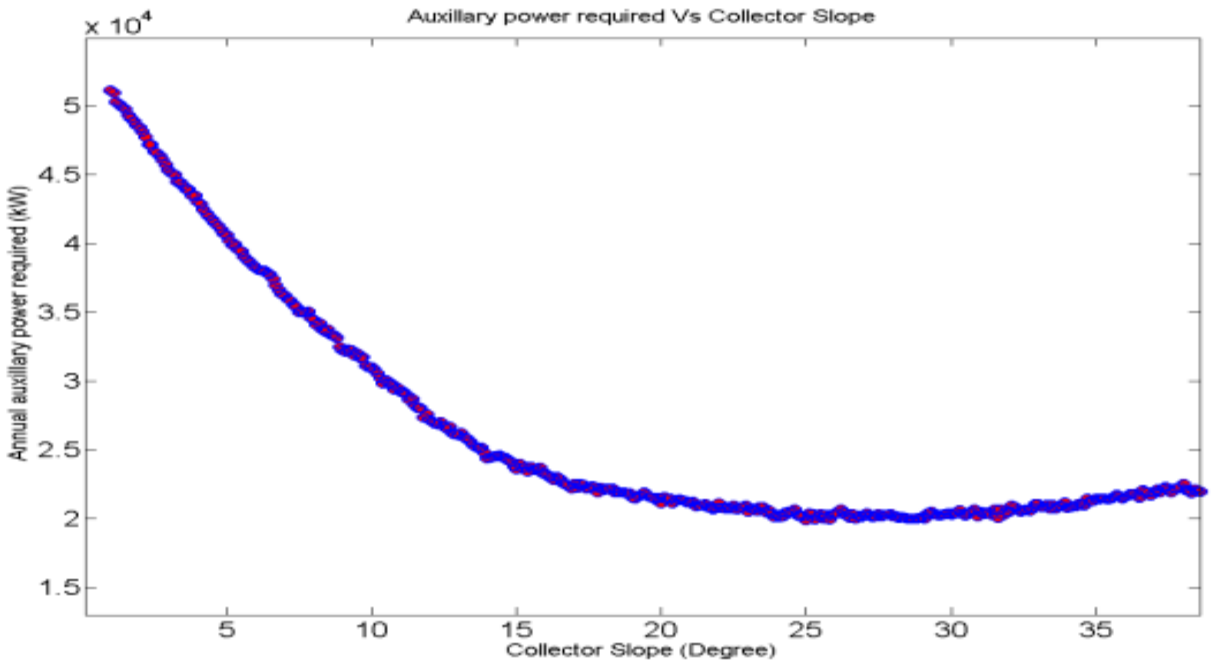

Figure 4.1.9: Annual auxiliary power required Vs Collector slope for New Delhi

Figure 4.1.10, shows the variation in auxiliary heater power required with change in collector slope for the city of Chennai. It can be seen that the minimum value for auxiliary heater power required is obtained for collector slope of around 13°. This through the iterations was precisely calculated to be 12.7°. This value is also close to the latitude of the city of Chennai i.e. 13.08°.

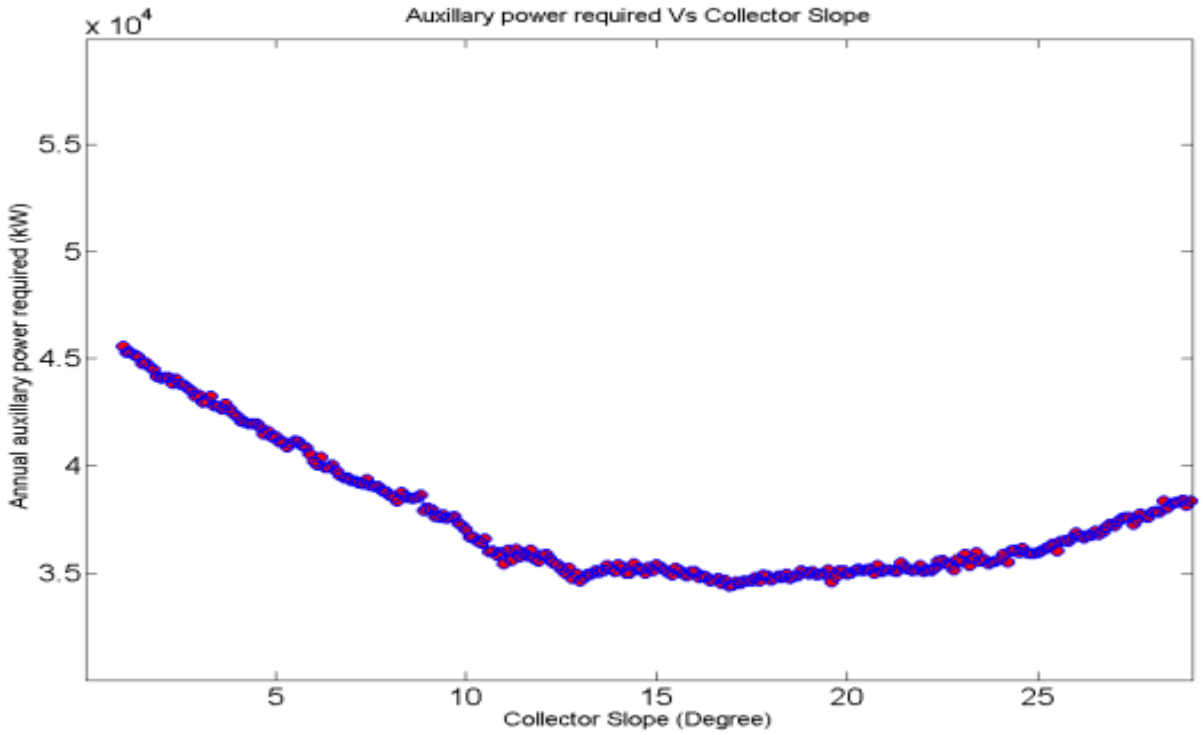

Figure 4.1.10: Annual auxiliary power required Vs Collector slope for Chennai

Similarly the optimum value of collector slope was calculated for the other two cities as well. The optimum value of collector slope for the selected cities can be seen in Table 4.1.2.

City	Optimum Collector Slope	Unit
Bangalore	11.2	Degree
New Delhi	28.1	Degree
Jodhpur	25.7	Degree
Chennai	12.7	Degree

Table 4.1.2: Optimized collector slope for selected cities

4.1.3 Storage tank volume

There is a difference in number of sun hours and working hours of office being simulated i.e. hours of cooling load for our simulation. This difference necessitates usage of storage of the solar energy for non-sun hours. It is for this purpose a storage tank is introduced into the system. Size of storage tank represents amount of energy it can store, hence time period for which it can provide

energy, independently. This was verified by the simulations that for a larger volume of storage tank, auxiliary heater kicked in much later than for lower tank volume, after sun hours. Although a larger volume of storage tank needs more time to completely charge itself, missing on more number of early load hours and storing energy more than what is required to supply the load after sun hours. Hence an optimum value of storage tank would be at which a minima if received in the trend of annual auxiliary heater power required over the parametric analysis of storage tank volume. This was confirmed by glancing at Figure 4.1.11, representing the trend of annual auxiliary power required during iterations by varying storage tank volume for the selected cities. For this analysis the storage tank volume is varied from $0m^3$ to 45 m^3.

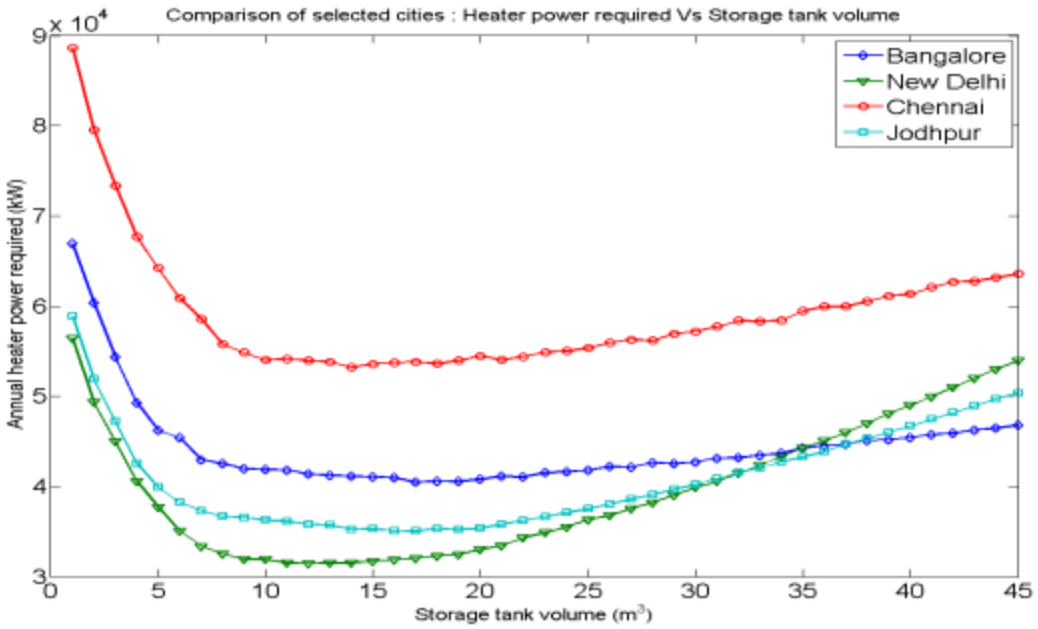

Figure 4.1.11: Annualheater power required Vs Storage tank volume for selected cities

Since at the optimum storage tank volume, minima can be seen in the trend of auxiliary heater power required and useful solar energy being inversely proportional, maxima should be seen in its trend. This can be observed in Figure 4.1.12 showing trend of annual useful solar energy during storage tank volume iterations. Similarly a peak can also be seen for trend of annual solar fraction in Figure 4.1.13

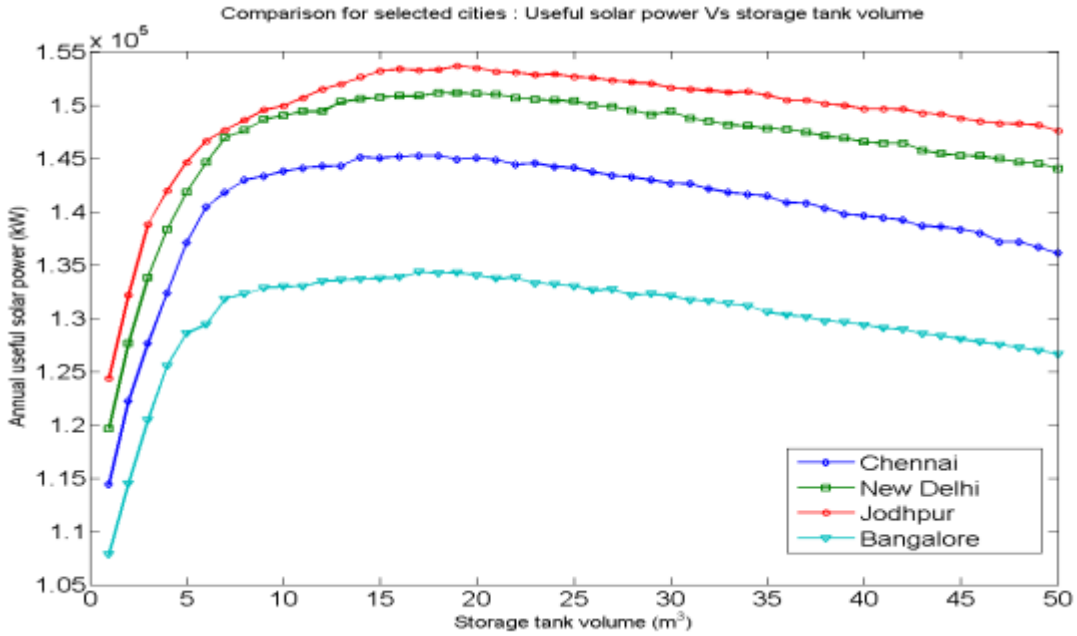

Figure 4.1.12: Annual solar power required VsStorage tank volume for selected cities

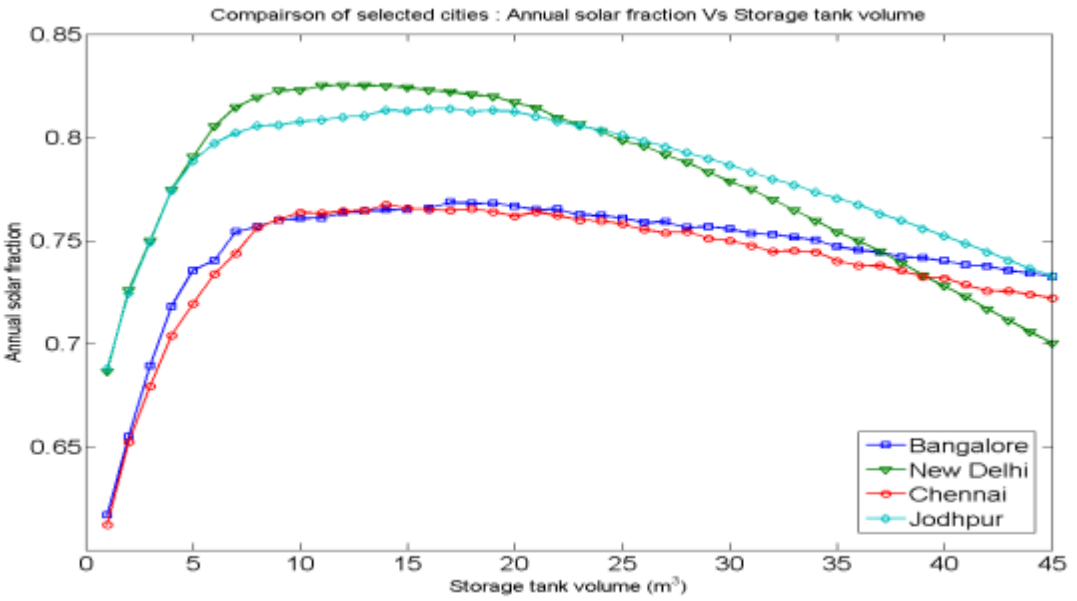

Figure 4.1.13: Annual solar fraction VsStorage tank volumefor selected cities

During these iterations, collector area was given a constant value of CA_{max} of respected cities. On further analysis it was found that on changing the collector area, points of minima and maxima for storage tank volume are different. Figures 4.1.14 and 4.1.15 represents trends of useful solar power required and solar fraction respectively. In each of these plots, the trends are plotted not just

for different storage tank volume but for various collector areas too. It can be seen in these plots that the peaks tend to shift towards higher value of storage tank volume with increasing collector area. That means the optimum value of storage tank is directly proportional to the collector area.

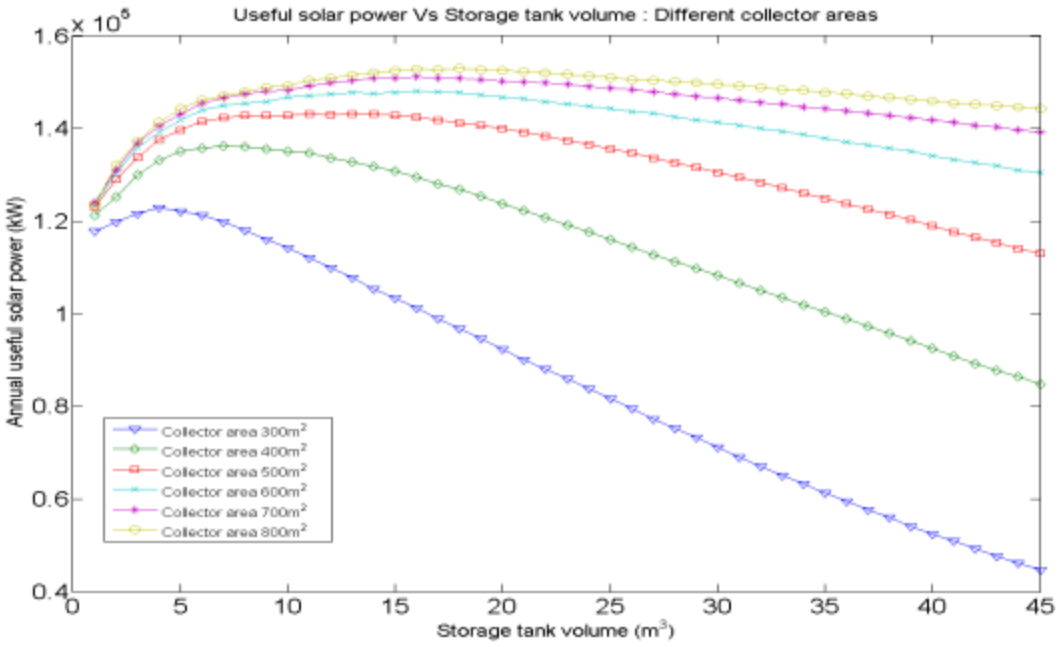

Figure 4.1.14: Annual useful solar power Vs Storage tank volume for different collector areas

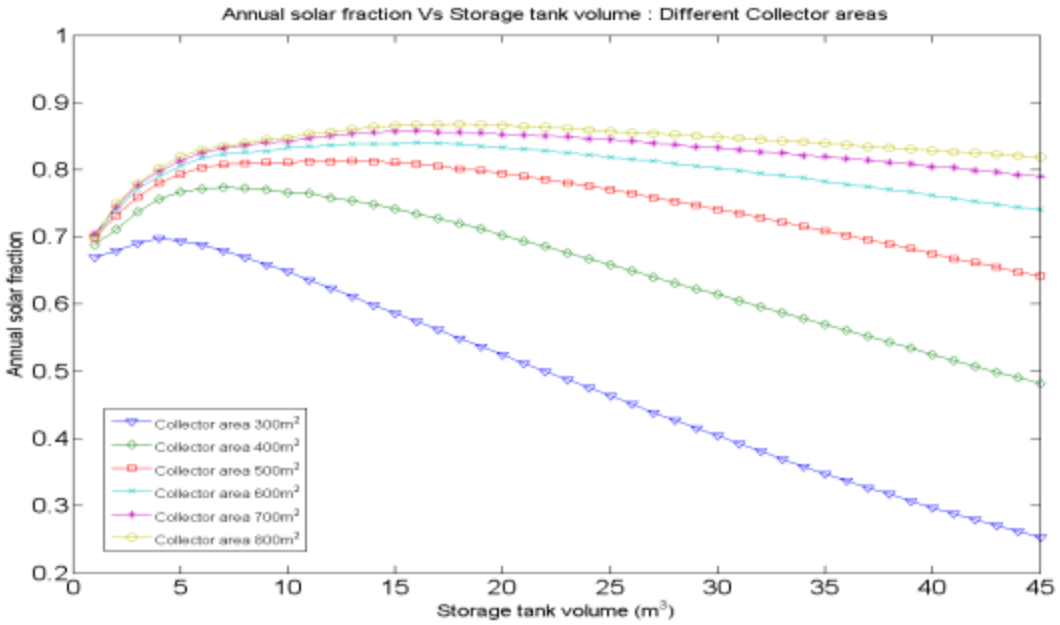

Figure 4.1.15: Annual solar fraction Vs Storage tank volume for different collector areas

This makes the optimum value of storage tank dependent on the optimum value of collector area. Since optimum value of collector area cannot be estimated through parametric analysis. It makes LCS analysis all the more important.

In parametric analysis, following was observed regarding the optimum values of the key parameters:

- The optimum value of collector area cannot be estimated by parametric analysis, as solar fraction is proportional to the parameter. Hence LCS analysisisrequired
- Optimum values of collector slope for each of the selected cities was found through parametric analysis. These are stated in Table 4.1.1
- Optimum value of storage tank can be found using the parametric analysis, but since it is dependent on optimum collector area. It could only be calculated after finding the optimum collector area through LCS analysis

4.2 Life Cycle Savings (LCS) Analysis

The method chosen to perform economic analysis for this thesis is life cycle savings method, which is presented in detail in Duffie and Beckman (1991). The life cycle cost savings method (LCS) has shown to be simple and practical method to derive the optimization function in terms of the basic costs of the system, the load, and the design parameters. Colle et.al (Colle, 2004) expressed the cost function LCS in terms of the solar collector area (A_c), the solar fraction (*f)*, the capital cost (C_a) and the auxiliary energy cost (C_E).

Let Q_L be the annual amount of heat required to drive the cooling cycle for a specified annual cooling capacity Qr. Neglecting the work of the pumps, the coefficient of performance of the thermally driven cycle is then defined by

$$COP = Qr/Q_L \qquad \text{Equation: 4.2.1}$$

Since, Q_L is the sum of the heat supplied by the auxiliary heater and solar collectors to the thermally driven system. The fraction of energy saved by the solar system is defined by $f=Qs/Q_L$ so that heat saved at the burner for a year period is $Qs=f*Q_L$. According to the $P_1 – P_2$ method given in Duffie and Beckman (1991), the cost savings related to the period of economical analysis

of N_e years, is expressed as the present value of the savings due to the operating cost minus the present value corresponding to the capital costs.

LCS defined in Duffie and Beckman is as follows:

$$LCS = P_1 C_{F1} Lf - P_2(C_a A_c + C_E) \qquad \text{Equation: 4.2.2}$$

Where P_1 is the ratio of the life-cycle fuel cost savings to the first-year fuel cost savings and P_2 is the ratio of the life-cycle expenditures incurred because of the additional capital investment to the initial investment. C_{F1} is the unit energy cost delivered from fuel, f is the solar fraction, L is the load, and hence first term is representing the savings due to fuel. Second term represents all additional expenditures incurred due to the collectors.

The above mentioned LCS equation is a basic equation in which any costs that are proportional to the fuel cost savings can be included by appropriate determination of P_1, and any costs that are proportional to the investment can be included in P_2. These modifications were done by Colle et.al.(Colle, 2004), during the specific case of economic analysis of solar based vapor absorption chiller.The LCS described by Colle et.al.is:

$$LCS = \frac{P_1 C_{E1} Q_r}{COP_{el}} - \frac{P_1 C_{F1} Q_r (1-f)}{COP} - P_2 (C_A A_C + C_E) - P_2 (C_{TH} - C_{EL} + \Delta C_{CT}) \qquad \text{Equation: 4.2.3}$$

Where the sum of first two terms corresponds to savings due to replacement of compression based AC by absorption chiller. The third term corresponds to capital cost of solar heating system, while the last term corresponds to difference of the capital cost between a compression based AC and that of an absorption chiller. Where, ΔC_{CT} is the difference between the costs of cooling towers.

The four terms on the right side equation 4.2.3 represent different components of the LCS function. They are as follows:

- The first term i.e. $\frac{P_1 C_{E1} Q_r}{COP_{el}}$ depicts the life term running costs of a compression AC (i.e electricity costs)
- Second term i.e.$\frac{P_1 C_{F1} Q_r (1-f)}{COP}$ depicts the life term running fuel cost of an absorption chiller (i.e heater fuel costs)
- Third term i.e.$P_2 (C_A A_C + C_E)$ depicts the life term investment costs of solar collectors
- Last term i.e.$P_2 (C_{TH} - C_{EL} + \Delta C_{CT})$ depicts the life difference in investment costs of absorption chiller and compression AC.

The terms P1 and P2 which are defined above can be calculated using equations 4.2.4 and 4.2.5, which are given below:

$P_1 = (1\text{-}C\bar{t})\ PWF(N_e, i_F, d)$ Equation: 4.2.4

$$P_2 = D + (1-D)\frac{PWF(N_{min},0,d)}{PWF(N_L,0,m)} - \bar{t}(1-D)\left[PWF(N_{min},0,d)\left(m - \frac{1}{PWF(N_L,0,m)}\right) + \frac{PWF(N_{min},0,d)}{PWF(N_L,0,m)}\right] + M_S\left(1-C\bar{t}\right) * PWF(N_e,i,d) + tV\left(1-\bar{t}\right) * PWF(N_e,i,d) - \frac{C\bar{t}}{N_D}PWF(N'_{min},0,d) - \frac{R_v}{(1+d)^{N_e}}(1-C\bar{t})$$ Equation: 4.2.5

The several terms represented in above mentioned equations, their values used for analysis, and the sources of the values can be read in Table 4.2.1. Values without source are the ones which can be dependent on individual choice such as years of loan, downpayment ratio, ratio of resale value etc.

Term	**Description**	**Value**	**Unit**	**Source**
C_{F1}	cost of auxiliary energy	6.03	INR/kWh	SRE, 2013
C_{E1}	cost of electric energy	6.7	INR/kWh	BESCOM, 2012
C_A	cost of collector per unit area	5000	INR/m2	Personal Conversation
C_E	installation and other minor cost of collector	100000	INR	Carrier, 2013
C_{EL}	capital cost of a 20 Ton AC	300000	INR	Carrier, 2013
C_{TH}	capital cost of VAM	400000	INR	S-CTT, 2013
COP_{el}	COP of carrier AC	2.5		Carrier, 2013
COP	COP of VAM	0.62		Simulation Result
C	flag indicating income producing or not	0		
i_F	fuel inflation rate	9	%	Ministry of Statics, GOI, 2013
d	discount rate	8	%	Ministry of Statics, GOI, 2013
m	annual mortgage rate	10.5	%	Ministry of

				Statics, GOI, 2013
i	general inflation rate	7	%	RBI, 2013
N_e	period of economic analysis	10	years	
N_L	term of loan	10	years	S-CTT, 2013
N_{min}	minimum of N_e and N_L	10	years	
N'_{min}	years over which depreciation contributes to analysis	5	years	S-CTT, 2013
N_D	depreciation lifetime	5	years	S-CTT, 2013
D	ratio of downpayment to initial investment	0.1		
M_s	ratio of first-year miscellaneous costs to initial investment	0.015		
V	ratio of assessed valuation of solar energy in first year to initial investment in system	0.55		
R_v	ratio of resale value at end of period of analysis to initial investment	0.05		

Table 4.2.1: Terms used in LCS analysis, their values, units, and sources

The LCS analysis was carried out for different values of collector area, for each of the selected cities. LCS function not only depends on financial parameters but also on the cooling load and solar fraction achieved at every simulation. Figure 4.2.1 shows values of LCS for varying collector areas. LCS trend shown in the plot seems to increase with increasing collector area till a certain value and then starts decreasing. This is the optimum value of collector area, where maximum savings is achieved. The LCS values were expected to be in the negative due to factors such as, higher capital cost for VAMs, higher auxiliary energy cost, lower electricity cost, no government subsidy, no carbon tax etc. Each of factors is responsible for the negative values of LCS. At first glance, LCS values being in six figured might be scary but the fact that these values are for 10 year period is important here. In Indian subcontinent 1, 00,000 is referred to as 1 Lakh in monetary terms. With optimum sizing of the collector the system faces a loss of 2.8 lakhs per year i.e. 2.8 $*10^5$ Indian Rupees, which reduces to 2 lakh per year if cost of VAM is taken as 4 lakh instead of

14 lakhs as seen in Figure 4.2.2. This brings into notice the impact decrease in capital cost of a single component can have on LCS function.

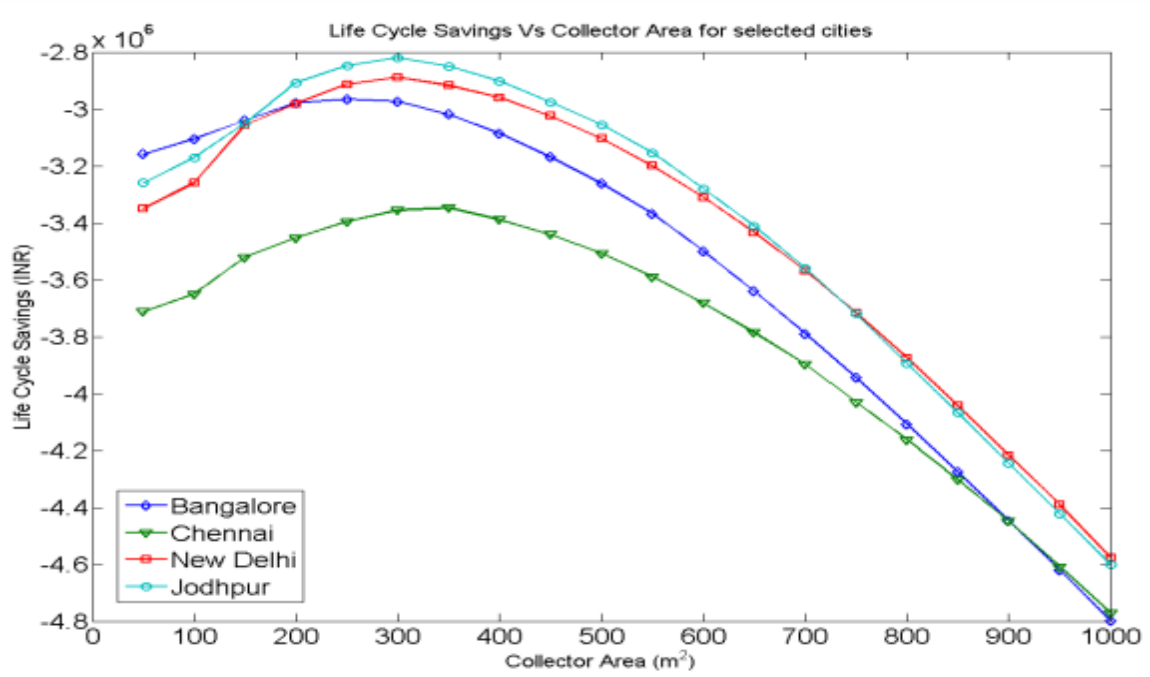

Figure 4.2.1: LCS Vs Collector area with VAM cost as 14 lakhs

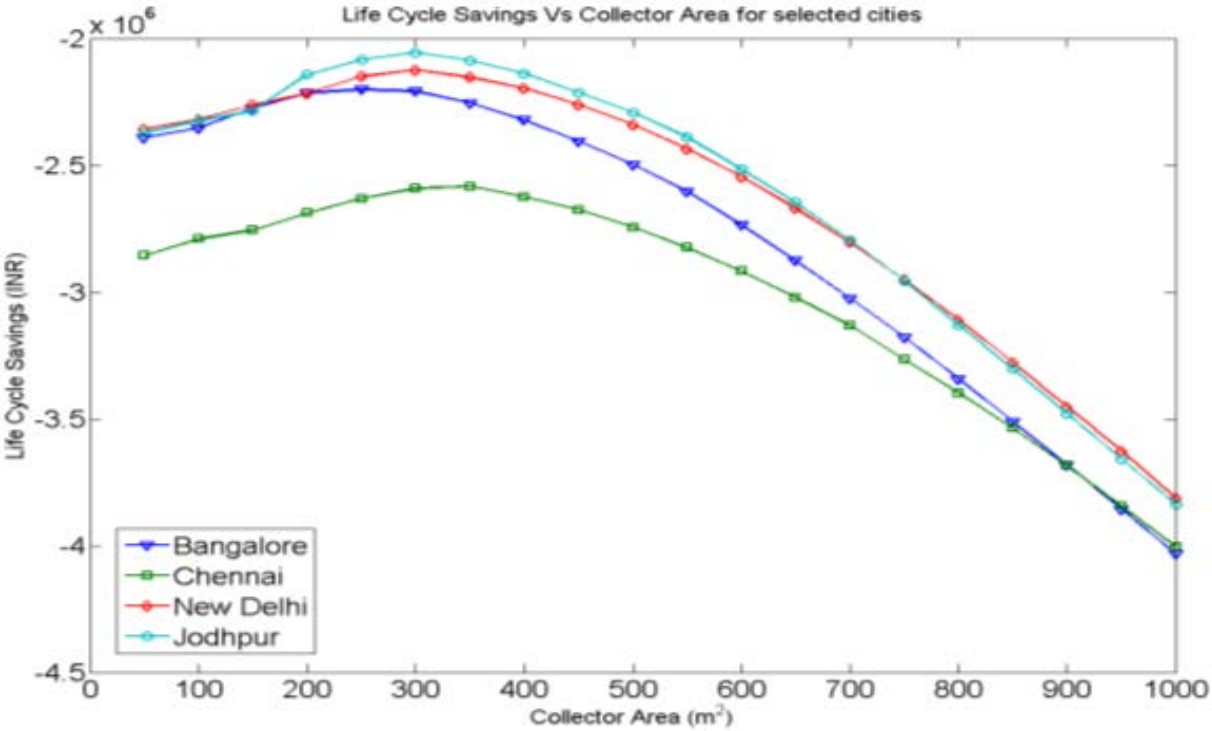

Figure 4.2.2: LCS Vs Collector area with VAM cost as 4 lakhs

The optimum collector areas for selected cities were the ones with highest value of LCS. After calculating the optimum collector areas, the parametric analysis was repeated with these collector areas and optimum storage tank volumes were calculated. These values are given in Table 4.2.2.

Chennai is the city with least solar irradiation among the selected cities, and highest cooling load requirement. For the months of September to March, Chennai has more cooling load requirement than even Jodhpur or New Delhi. This low irradiation and high load can be considered as the reason behind Chennai being the city with highest value for optimum collector area. On comparing optimum values for Jodhpur and Chennai, it is noticed that although both cities have same optimum value of storage tank, the optimum value of collector area is 70 m^2 lower for Jodhpur. This can be attributed to the fact that Jodhpur has more solar irradiation than Chennai, which makes the collectors gain more energy per unit area.

City	Optimum collector area (m^2)	Optimum storage tank volume (m^3)
Bangalore	320	7
New Delhi	320	8
Jodhpur	290	10
Chennai	360	10

Table 4.2.2: Optimum values of collector area and storage tank volume for selected cities

5.0 Conclusion

The primary objective of this study was to simulate and then optimize a solar based on absorption refrigeration system assisted by solar energy and an auxiliary heater for Indian cities. Cities were selected such that they represent different climatic regions of India and have different incident solar irradiation. The solar based absorption system consists of several components and several control strategies can be implemented to optimize the system. Considering the time available for this study, scope of this work was constricted to the optimization of three key parameters i.e. Collector area, Collector slope, and Storage tank volume.

Demand for air conditioning for selected cities was modelled using TRNBuild, a module of TRNSYS. TRNBuild allows the simulation of cooling loadthrough dynamic analysis of various input parameters and weather conditions, rather than simple recognizable patterns of load profiles with simplifying assumptions. The load calculated was then provided as an input to the simulation of solar based absorption system, which was done using TRNSYS.

The results obtained from the parametric optimization and Life Cycle Savings analysis of the simulated solar based absorption system, indicate that with an area of 320 m^2 of evacuated tube collectors with an inclination of 28.1° and 8 m^3 of storage tank is the optimum configuration of the key parameters for the city of New Delhi, maximizing the gain of useful energy of the system and minimizing the consumption of auxiliary energy. Similarly the optimum configurations were also calculated for the other selected cities. The optimum configuration of selected cities can be seen in Table 5.1.

	OptimizedValues		
City	Collectorarea (m2)	Collectorslope (Degree)	Storage tankvolume (m3)
New Delhi	320	28.1	8
Jodhpur	290	25.7	10
Bangalore	320	11.2	7
Chennai	360	12.7	10

Table 5.1 Optimum configuration of key parameters for selected cities

Through successful simulation and optimization of the solar based absorption system for Indian cities, the objective of this study was successfully achieved. The developed simulation model can be used in future woks to perform thermoeconomic optimization of the similar system. This model can be used to study the variation of other parameters which were outside the scope of this work, such as, different sizes of absorption chiller, variable flow pumps, different climates, and different thermostat settings.

As stated earlier that existing absorption chiller model in TRNSYS is relying on only energy balance and mass balance, between the entering and exiting water streams. Due to which the model is unable to depict the dependence of the performance of an absorption chiller on key parameters like hot water inlet temperature, hot water inlet flow rate, and chilled water outlet setting temperature. In practice an absorption chiller´s performance decreases if the temperature of hot water inlet is decreased, whereas in the TRNSYS model the performance remains same. In this thesis to negate this effect, the hot water inlet temperature to the absorption chiller is controlled using thermostat so that it doesn´t fall below a specified minimum value. In future, to make the simulation results more realistic, a new absorption chiller model in TRNSYS could be written.

Future optimization studies on solar based absorption system could also be conducted on different control strategies which could be implemented in this system. Control strategies could be put in place in the cooling water loop to vary the cooling water circulation based on the input load at absorption chiller. Another area of future study could be the environmental impact of a solar based absorption system, quantifying the positive impact in terms of CO2 reduction.

Annexure I

TRNSYS can only be used to run a specific simulation for input parameters. Since this study required parametric analysis of these input parameters, iterations with varying inputs were required. To simplify the task of running the software a large number of times, and performing calculations with the outputs, MATLAB was used.

The following is the MATLAB code used to perform iterations and the necessary calculations. This code was changed for specific parametric analysis during the study, and further extended to include the Life Cycle Savings (LCS) analysis.

```
clc;

%Technical Parameters
Coll_Area = 980; %Unit: m2
Coll_Slope = 12.98; %Unit: DegC
Vol_Stor_Tank = 14; %Unit: m3
Sim_Start_Time = 0; %Unit: hours
Sim_Stop_Time = 8760; %Unit: hours
Sim_Time_Step = 1; %Unit: hours
Coll_Flowrate = (Coll_Area/980)*15000; %Unit: kg/hr
AH_Kick_In_Temp = 80; %Unit: DegC
AH_Set_Point_Temp = 80; %Unit: DegC

%Economic Parameters
C_F1 = 6.03; %cost of auxillary energy
C_E1 = 6.7; %cost of electric energy
```

```
C_A = 5000; %cost of collector per unit area

C_E = 100000; %installation and other minor cost of collector

C_EL = 300000; %capital cost of AC of same capacity

C_TH = 400000; %capital cost of VAM

COP_el = 2.5; %cop of carrier AC

COP = 0.62; %cop of VAM

C = 0; %flag indicating income producing or non-income producing

i_F = 9; %fuel inflation rate

d = 8; %discount rate

m = 10.5; %annual mortgage rate

i = 7; %general inflation rate

N_e = 10; %period of economic analysis

N_L = 10; %term of loan

N_min = 10; %min of N_e and N_L

Nd_min = 5; %years over which depreciation contributes to analysis

N_D = 5; %depreciation lifetime

t = 0.02; %property tax rate

t_bar = 0.45; %income tax rate

D = 0.1; %ratio of down payment to initial investment

M_S = 0.015; %ratio of first year maintenance costs to initial investment

V = 0.55; %ratio of assessed valuation of solar energy system in first year to initial investment

R_v = 0.05; %ratio of resale value at the end of period of analysis

D_CT = 200000; %Delta cooling tower cost
```

```
% Technical Iterative Parameters
for loop = 1:1:20
    %Writing file
    inputData = struct;
    inputData.V_ST = Vol_Stor_Tank;
    inputData.C_Area = loop*50;
    inputData.C_Slope = Coll_Slope;
    inputData.S_Start_Time = Sim_Start_Time;
    inputData.S_Stop_Time = Sim_Stop_Time;
    inputData.S_Time_Step = Sim_Time_Step;
    inputData.C_Flowrate = Coll_Flowrate;
    inputData.AH_KTemp = AH_Kick_In_Temp;
    inputData.AH_STemp = AH_Set_Point_Temp;
    writeTRNSYSinput(inputData,'D:\Dev_intern\');

    %run TRNSYS model%
    [~, ~] = system('"C:\Trnsys17\Exe\TRNExe.exe" "D:\Dev_intern\SBAC-1_Matlab.dck" /n');
    %[~, ~] = system('"C:\Trnsys17\Exe\TRNExe.exe" "D:\Dev_intern\SBAC-1.dck" /n');

    data_WS = dlmread('D:\Dev_intern\SBAC-1_Matlab.out',',',1,0);

     sf(loop) = data_WS(8761,2);
     Q_r(loop) = data_WS(8761,3);
%       ap_m(i) = data_WS(8761,4);
```

```
        sp_m(i) = data_WS(8761,5);

       A_C = loop*50;


    %Economic Iterations

    P1 = (1-C*t_bar)*pwf_f(N_e,i_F,d);

    P2 = D + (1-D)*(pwf_f(N_min,0,d)/pwf_f(N_L,0,m))-t_bar*(1-D)*(pwf_f(N_min,0,d)*(m-(1/pwf_f(N_L,0,m)))+(pwf_f(N_min,0,d)/pwf_f(N_L,0,m)))+M_S*(1-C*t_bar)*pwf_f(N_e,i,d)+t*V*(1-t_bar)*pwf_f(N_e,i,d)-((C*t_bar)/N_D)*pwf_f(Nd_min,0,d)-(R_v/((1+d)^N_e))*(1-C*t_bar);

    A1(loop) = (P1*C_E1*Q_r(loop))/(COP_el);

    A2(loop) = (P1*C_F1*Q_r(loop)*(1-sf(loop)))/COP;

    A3(loop) = P2*(C_A*A_C+C_E);

    A4(loop) = P2*(C_TH-C_EL+D_CT);

    LCS(loop) = A1(loop) -A2(loop) -A3(loop) -A4(loop);

    var(loop) = loop*50;

    sav_d(loop) = LCS(loop);

end

 for i=1:1:12

    sf_m(i) = data_WS(1+i*730,2); %monthly average of solar fraction

    Q_m(i) = data_WS(1+i*730,3)/30; %this is the load in kWh per day average over a month

     t_amb_m(i) = data_WS(1+i*730,4); % monthly average ambient temperature

     DNI_m(i) = data_WS(1+i*730,5)/30; % monthly average of daily DNI for a location in kWh

 end
```

Bibliography

Al-Karaghouli, A., Abood, I., Al-Hamdani, N.I., 1991. The solar energy research center building thermal performance evaluation during the summer season. Energy Conversion and Management 32, 409–417.

Assilzadeh, F., Kalogirou, S.A (2005), Simulation and optimization of a LiBr solar absorption cooling system with evacuated tube collectors, Renewable Energy 30 , 1143-1159

Balaras, C.A., Grossman, G., Henning, H.M., Ferreira, C.A.I., Podesser, E., Wang, L., Wiemken, E., 2007. Solar air conditioning in Europe – an overview. Renewable and Sustainable Energy Reviews 11, 299–314.

Bangalore Electricity Supply Company Ltd (BESCOM), Electricity tariff – 2013, K.E.R.C Order Dated 30.04.2012

Best, R., Ortega, N., 1999. Solar refrigeration and cooling. Renewable Energy 16, 685–690.

Bong, T.Y., Ng, K.C., Tay, A.O., 1987. Performance study of a solar powered air conditioning system. Solar Energy 39 (3), 173–182.

De-centralised Energy Technologies (DET) Purchase Order (PO), Purchase order of same capacity VAM at SIEMENS, Bangalore, India, 2011

Duff, W.S., Winston, R., O'Gallagher, J.J., Bergquam, J., Henkel, T., 2004. Performance of the Sacramento demonstration ICPC collector and double effect chiller. Solar Energy 76, 175–180.

Duffie, J.A., Beckman, W.A., 1991. Solar Engineering of Thermal Processes, second ed. John Wiley, New York.

Eicker, U., Pietruschka, D. (2009), Optimisation and economics of solar cooling systems, Advances in building energy research, 2009, Volume 3, Pages 45-82 ISSN: 1751-2549

Florides, G.A, Kalogirou, S.A, Tassou, S.A, and Wrobel, L.C (2002), Modelling and simulation of an asborption solar cooling system for Cyprus, Solar Energy Vol 72, pp 43-51

Ghaddar, N.K, Shibab, M. and Bdeir, F. (1997) , Modelling and simulation of solar absorption system performance in Beirut, Renewable Energy 10 (4) , 539-558

Hattem, D.V., Dato, P.A., 1981. Description of an active solar cooling system, using a LiBr–H2O absorption machine. Energy and Buildings 3, 169–196.

Henning, H.M. (Ed.), 2007. Solar-Assisted Air-Conditioning in Buildings, A Handbook for Planners, second ed. Springer, Wien, New York.

Jesko, Z. (2008), Classification of solar collectors, Engineering for rural development, Jelgava, 29-30.05.2008

K4RES-H, 2006. Solar Assisted Cooling-State of the Art, Key Issues for Renewable Heat in Europe, Solar Assisted Cooling-WP3, Task 3.5, Contract EIE/04/204/S07.38607, 21p.

Kim, D.-S., 2007. Solar Absorption Cooling. Ph.D. Dissertation, Delft University of Technology, Netherlands.

Li, Z.F., Sumathy, K., 2001. Experimental studies on a solar powered air conditioning system with partitioned hot water storage tank. Solar Energy 71 (5), 285–297.

Lokurlu, A., Mu¨ ller, G., 2005. Experiences with the worldwide first solar cooling system based on trough collectors combined with double effect absorption chillers. In: Proceedings of the International Conference on Solar Air-conditioning, Bad Staffelstein, Germany.

Meza, J.I., Gonza´lez, J.E., Khan, A.Y., 1998. Experimental assessment of a solar assisted air conditioning system for applications in Puerto Rico. In: ASME Proceedings of the Solar Energy Division 8, pp. 149–154.

Ministry of Statistics and Program Implementation, Government of India, Press Release, Consumer price index numbers on base 2010=100 for rural, urban and combined for the month of May, 2013

MNRE, Chapter 1 - Fundamentals of Solar Energy, 2012

Mukherji B, et al. In India, weak monsoon adds to power crisis. Wall Street Journal, World section, India subsection, online edition (2 Aug 2012)

NREL, Solar resource map of India, 2010

Pe´rez, R.A., 2007. Heat and Mass Transfer Effects in Air-Cooled Vertical Tube Absorbers. M.Sc. Thesis, University of Puerto Rico – Mayaguez Campus.

Pongtornkulpanich, A., Thepa,S. , Amornkitbamrung, M, Butcher,C. (2007), Experience with fully operational solar-driven 10-ton LiBr/H2O single-effect absorption cooling system in Thailand, Renewable Energy, Volume 33, Issue 5, pages 943-949

Reserve Bank of India (RBI), Speech by Deepak Mohanty, Executive Director of Reserve Bank of India, Mumbai, January 31st, 2013

Safarik, M., Richter, L., Mockel, F., Kretschmar, S., 2005. Performance data of a small capacity absorption chiller. In: Proceedings of the International Conference on Solar Air-conditioning, Bad Staffelstein, Germany.

Sargoy Ishaya, Solar Cooling – Methods and Applications, U.S. Green Building Council Summit, California, 2011

Sayigh, A.A.M., Saada, M.K., 1981. A three and a half ton solar air conditioner's performance in Riyadh, Saudi Arabia. In: Proceedings of the International Solar Energy Society Congress, Brighton, vol. 1, pp. 537–543.

Siemens Real Estate (SRE), Data acquired in person, Bangalore,India, 2013

Sivak M. Potential energy demand for cooling in the 50 largest metropolitan areas of the world: implications for developing countries. Energy Policy 37(4):1382-1384 (2009)

Storkenmaier, F., Harm, M., Schweigler, C., Ziegler, F., Albers, J., Kohlenbach, P., Sengewald, T., 2003. Small-capacity water/LiBr absorption chiller for solar cooling and waste-heat driven cooling. In: Proceedings of the International Congress of Refrigeration, Washington, DC, USA.

Syed, A., Izquierdo, M., Rodriguez, P., Maidment, G., Missenden, J., Lecuona, A., Tozer, R., 2005. A novel experimental investigation of a solar cooling system in Madrid. International Journal of Refrigeration 28, 859–871.

Vidal, H, Escobar, R. and Colle, S. (2009), Simulation and optimization of a solar driven air conditioning system for a house in Chile, ISES Solar World Congress

Ward, D.S., Lo¨ f, G.O.G., 1975. Design and construction of a residential solar heating and cooling system. Solar Energy 17 (1), 13–20.

Ward, D.S., Lo¨ f, G.O.G., Uesaki, T., 1978. Cooling subsystem design in CSU solar house III. Solar Energy 20 (2), 119–126.

Ward, D.S., Weiss, T.A., Lo¨ f, G.O.G., 1976. Preliminary performance of CSU Solar House I heating and cooling system. Solar Energy 18 (6), 541–548.

World Bank, 2008, Residential consumption of electricity in India, Documentation of Data and Methodology.

Qu, Ming, et.al, Performance modeling of a solar driven absorption cooling system for Carnegie mellon university's intelligent workplace, Renewable Energy Resources and a Greener Future Vol. VIII-7-5

Yeung, M.R., Yuen, P.K., Dunn, A., Cornish, L.S., 1992. Performance of a solar powered air conditioning system in Hong Kong. Solar Energy 48 (5), 309–319.

Zambrano, D., Bordons, C., Garcia-Gabin, W., Camacho, E.F., 2007. Model development and validation of a solar cooling plant. International Journal of Refrigeration. doi:10.1016/ j.ijrefrig.2007.05.00.